AD-A172 284 CALCULATION OF THE VIBRONIC STRUCTURE OF SOLUTE/SOLVENT VAN DER WAALS CLU..(U) COLORADO STATE UNIV FORT COLLINS DEPT OF CHEMISTRY J A MENAPACE ET AL. 01 JUN 86 TR-22 1/1

UNCLASSIFIED N00014-79-C-0647 F/G 7/4 NL

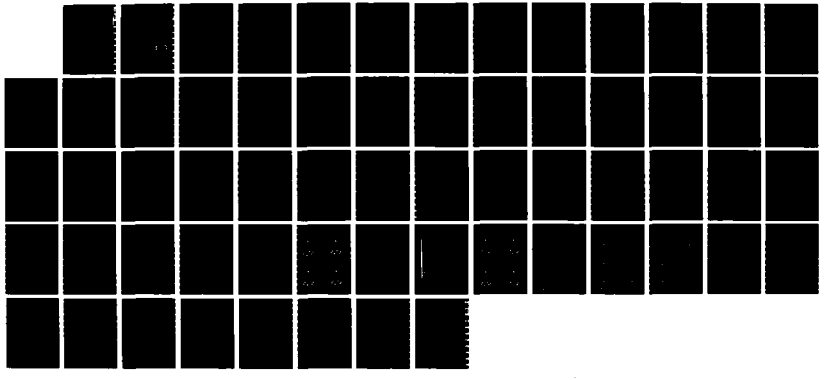

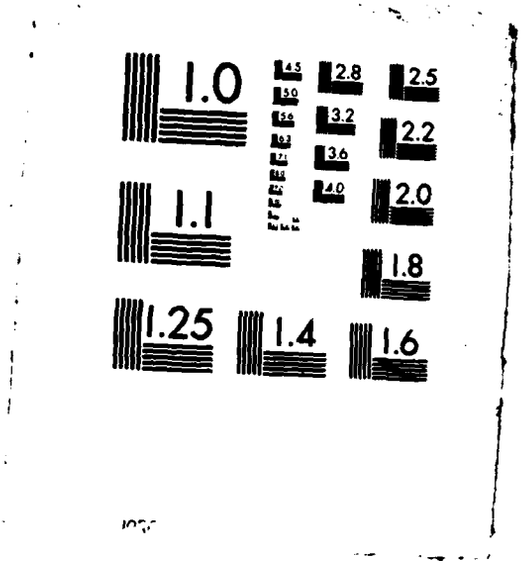
1.0
1.1
1.25
1.4
1.6
1.8
2.0
2.2
2.5
2.8
3.2
3.6
4.0
4.5
5.0
5.6
6.3

(12)

OFFICE OF NAVAL RESEARCH

Contract N00014-79-C-0647

TECHNICAL REPORT #22

"CALCULATION OF THE VIBRONIC STRUCTURE OF SOLUTE/ SOLVENT van der WAALS CLUSTERS"

by

J.A. Menapace and E.R. Bernstein

Prepared for Publication
in the Journal of Chemical Physics of the
Conference Proceedings of the
191th ACS National Meeting, New York, 1986

Department of Chemistry
Colorado State University
Fort Collins, Colorado 80523

1 JUNE
~~May~~ 1986

UNCLASSIFIED

SECURITY CLASSIFICATION OF THIS PAGE

REPORT DOCUMENTATION PAGE

1a. REPORT SECURITY CLASSIFICATION	1b. RESTRICTIVE MARKINGS AD-A172 287
2a. SECURITY CLASSIFICATION AUTHORITY	3. DISTRIBUTION / AVAILABILITY OF REPORT Approved for public release; distribution unlimited.
2b. DECLASSIFICATION / DOWNGRADING SCHEDULE Unclassified	
4. PERFORMING ORGANIZATION REPORT NUMBER(S) N00014-79-C-0647	5. MONITORING ORGANIZATION REPORT NUMBER(S)
6a. NAME OF PERFORMING ORGANIZATION Colorado State University	6b. OFFICE SYMBOL (If applicable)
6c. ADDRESS (City, State, and ZIP Code) Department of Chemistry Fort Collins, Colorado 80523	7a. NAME OF MONITORING ORGANIZATION
8a. NAME OF FUNDING / SPONSORING ORGANIZATION U.S. Army Research Office	8b. OFFICE SYMBOL (If applicable)
8c. ADDRESS (City, State, and ZIP Code) Post Office Box 12211 Research Triangle Park, NC 27709	7b. ADDRESS (City, State, and ZIP Code)
	9 PROCUREMENT INSTRUMENT IDENTIFICATION NUMBER N00014-79-C-0647
	10 SOURCE OF FUNDING NUMBERS: PROGRAM ELEMENT NO. / PROJECT NO. / TASK NO. / WORK UNIT ACCESSION NO.

11. TITLE (Include Security Classification)
"Calculation of the Vibronic Structure of Solute/Solvent van der Waals Cluster"

12. PERSONAL AUTHOR(S)
J.A. Menapace and E.R. Bernstein

13a. TYPE OF REPORT	13b. TIME COVERED	14. DATE OF REPORT (Year, Month, Day)	15 PAGE COUNT
Technical Report	FROM _____ TO _____	June 1, 1986	58

16. SUPPLEMENTARY NOTATION The view, opinions, and/or findings contained in this report are those of the author(s) and should not be construed as an official Department of the Army position, policy, or decision, unless so designated by other documentation.

17. COSATI CODES			18. SUBJECT TERMS (Continue on reverse if necessary and identify by block number)
FIELD	GROUP	SUB-GROUP	

19. ABSTRACT (Continue on reverse if necessary and identify by block number)

Calculations of the eigenvectors and eigenvalues for the van der Waals clusters benzene$(Ar)_1$, $(CH_4)_1$, $(H_2O)_1$, and $(NH_3)_1$, and s-tetrazine$(Ar)_1$ are presented. The calculations are based on an atom-atom Lennard-Jones (6-12-1-10-12) potential function, which includes hydrogen bonding, and a normal coordinate analysis. The clusters are treated as giant molecules. The results of these calculations are then used to assign the van der Waals vibronic spectra of the above clusters. Agreement between calculations and experiments is excellent for binding energies, symmetries, and van der Waals frequencies. The $S_2 \leftarrow S_1$ vibronic transitions of the above clusters are essentially completely assigned based on these calculations. A major conclusion of this work is that the low frequency van der Waals torsions and bends are active in Herzberg-Teller vibronic coupling. A number of approximate diatomic molecule calculations are compared to the above procedure and thereby evaluated.

20. DISTRIBUTION / AVAILABILITY OF ABSTRACT	21 ABSTRACT SECURITY CLASSIFICATION
☒ UNCLASSIFIED/UNLIMITED ☐ SAME AS RPT ☐ DTIC USERS	UNCLASSIFIED
22a. NAME OF RESPONSIBLE INDIVIDUAL Elliot R. Bernstein	22b TELEPHONE (Include Area Code) 303-491-6347 / 22c. OFFICE SYMBOL

DD FORM 1473, 84 MAR 83 APR edition may be used until exhausted. All other editions are obsolete.

SECURITY CLASSIFICATION OF THIS PAGE

UNCLASSIFIED

I. Introduction.

The combination of laser spectroscopy and supersonic molecular jet expansions has made possible the study of a wide array of weakly bound van der Waals (vdW) molecules in the gas phase. These clusters, formed in the jet expansion, are stable in the post-expansion region and can be studied as isolated molecules. They are interesting both theoretically and experimentally because of their unique characteristics such as low binding energies, large intermolecular equilibrium distances, and low frequency intermolecular vibrational vdW modes. Furthermore, the vdW clusters only slightly perturb the individual properties of their molecular constituents.[1] These characteristics set the vdW cluster apart as a distinct phase of matter to be explored and understood.

The electronic-vibrational spectroscopy of aromatic molecules like benzene[2-4] and s-tetrazine[5] clustered with various solvents reveals interesting information regarding unique cluster characteristics. Specifically, the studies show detailed information pertaining to the intermolecular energetics and dynamics of cluster interactions, especially in the area of the clusters' low-frequency vdW vibrational modes. These modes are of considerable interest since they represent the precursors of a variety of condensed phase eigenstates such as phonons in liquids and solids. They are also key factors in cluster dynamics as they play a major role in the energy transfer processes of intramolecular vibrational redistribution (IVR) and vibrational predissociation (VP).

Presently, little information is available concerning the detailed energetics of vdW modes either experimentally or theoretically. The theoretical work on cluster energetics and dynamics, to date, treats only the vdW stretching mode.[1,6,7] In these studies, the clusters are treated using a "dumbbell" approximation in which the intermolecular motion is restricted to a stretching mode form. Within this approximation, the neglect of bending and/or

torsional vdW modes seriously limits the application of existing theoretical treatments to IVR and VP phenomena occurring in molecule-molecule type clusters. The stretching mode restriction dictates that only certain energy transfer processes can occur, specifically, those which involve the vdW stretch. Experimental evidence of the theory's limitation[4] is borne out in the observation of energy transfer from prepared states tangential to the vdW stretching motion. Part of the difficulty of incorporating the vdW bending and/or torsional modes into the theory is that no model has been developed to describe either their energetics or mode nature.

In previous publications,[8] we have used theoretical calculations to elucidate structure and binding energy in the vdW cluster ground state. Combining these calculations with experimental observables such as binding energies, ionization energies, spectral shifts, relative feature intensities, and the appearance of cluster constituent, symmetry forbidden transitions has aided considerably in spectral assignment and understanding. The calculations always yield results consistent with experimental observations in regard to the number of cluster configurations observed, their respective binding energies, and their qualitative geometries.

In the majority of the cluster spectra studied, vdW vibronic features are observed and sometimes assigned based upon overtone and combination band analysis. In other cases, however, these vibronic features are numerous and complex, making elucidation of the mode fundamentals difficult and sometimes impossible. The vdW vibronic feature assignments have been made based upon the assumptions that the vdW stretch occurs at higher frequency and with greater intensity than vdW bends and torsions. Assigning spectra using these assumptions is a difficult task without *a priori* knowledge of vibronic mode nature since one must consider that, in nonlinear polyatomic molecule-molecule clusters, six vdW modes exist of which only one is a stretching mode. (In a non-linear atom-polyatomic molecule cluster, three vdW modes exist).

The studies reported in this publication involve the calculation of a complete set of ground state vdW vibrational modes for benzene$(Ar)_1$, s-tetrazine$(Ar)_1$, benzene$(CH_4)_1$, benzene$(H_2O)_1$, and benzene$(NH_3)_1$. The calculations are performed using a self-consistent pairwise atom-atom intermolecular potential developed by Scheraga, et al.[9] containing general nonbonding (6-12), general hydrogen bonding (10-12), and monopole charge parameters. The calculated ground state vdW modes are compared with cluster vibronic spectra previously studied in this[2,3] and other laboratories.[5] Consequently, a number of spectral reassignments are suggested. Vibronic selection rules governing the vdW cluster $S_1 \leftarrow S_0$ transition are also derived based upon calculated ground state cluster mode symmetry, cluster geometry and experimental observation. Within this framework, ramifications of Herzberg-Teller vibronic coupling are discussed as they pertain to experimental observations of Franck-Condon forbidden transitions.

The calculated vdW vibrations are presented for all systems considered as eigenvector normal modes and eigenvalue energies determined via normal coordinate analysis of the entire vdW cluster.[10] In performing the calculations, the high frequency intramolecular vibrations of the cluster constituents are assumed to be completely uncoupled from the low frequency vdW modes.

Simpler models are also considered in studying the vdW vibrations of benzene$(Ar)_1$. This system is studied using four methods: (1) a Taylor series expansion of the intermolecular vdW potential along the three Cartesian axes in which the term coefficients are related to the vibrational frequencies in these directions; (2) a Morse potential fit to the intermolecular vdW potential along each of the three Cartesian axes; (3) a Morse potential fit to the intermolecular vdW potential using $\beta = \frac{6}{R_o}$;[1,6,7] and (4) a semi-classical energy level fit to the intermolecular vdW potential using the JWKB method. These studies are presented to show the consistency of the calculations and to reveal

the advantages and pitfalls of the models. The four models involve treating the vdW clusters as simple two particle systems whose motions are restricted to the principle axes of the Cartesian coordinate system. The intermolecular vdW potential surfaces are thereby reduced to one-dimensional potential functions which can be analyzed in a diatomic molecule approximation.

The above outlined approaches are all based more or less on a rigid molecule, bound potential energy well approximation. This approach would seem quite reasonable for the stretching(s) and bending (b_x and b_y) degrees of freedom which are essentially translations of the components of the vdW molecules with respect to one another. Torsional modes (t_x, t_y, t_z), on the other hand, could in principle be modeled by a free/hindered rotor formalism.[11,12] A one dimensional "free rotor" description has been applied to the symmetry axis (z) torsional motion of benzene and toluene $(CH_4)_1$, $(CD_4)_1$ and $(CF_4)_1$ and compared to the experimental observations. Preliminary results suggest that this approach does not faithfully reproduce the experimentally observed spectra for this "isotopic" series in terms of line shapes, intensities, major features, and the number of observed transitions. A three dimensional "free rotor" model has also been applied to this problem in order to treat all torsional modes (t_x, t_y, t_z) simultaneously. Similar difficulties are experienced in fitting the experimentally observed spectra. An account of these studies will be submitted for publication in the near future.

The driving motivation in these studies is to answer the following questions: (1) if parametric calculations involving cluster geometry and binding energy are consistent with experiment, can the same data set be utilized to calculate intermolecular vibrational modes; and (2) what are the

advantages and pitfalls of the various models in regard to the complexity of calculation, the approximations made, and the nature of the results obtained?

II. Experimental Procedures.

Experimental data pertaining to the benzene$(Ar)_1$ vdW vibronic spectrum are obtained employing the experimental apparatus and procedures similar to those used previously to study vdW clusters.[8] The benzene$(Ar)_1$ S_1 S_o spectrum is recorded using a pulsed supersonic molecular jet expansion in combination with 1-color time-of-flight mass spectroscopy (TOFMS). A single Nd^{+3}/YAC pumped LDS 698 dye laser whose output is frequency doubled and then mixed with the Nd^{+3}/YAG 1.064 m fundamental is used to probe the 6^1_o region of the benzene$(Ar)_1$ cluster. A 5% Ar in He mixture is placed inline with liquid benzene in a trap maintained at room temperature. This three component gas mixture is then expanded using a pulsed nozzle maintained at 100 psig backing pressure. Apparatus chamber pressure is maintained at or below 4×10^{-6} torr during the experiment.

III. Theoretical Considerations.

The normal coordinate analyses of the vdW clusters are conducted employing the GF methods of Wilson.[10] These methods involve solving the characteristic equation of 3N-6 coupled harmonic oscillators for its 3N-6

non-zero eigenvalues and eigenvectors. The approach is to treat the vdW cluster as a "giant molecule" and treat both the intramolecular vibrational modes and the intermolecular vdW modes simultaneously. The intermolecular vdW potential field used in the analyses is expressed in an intermolecular symmetry coordinate system. In this coordinate system, the intermolecular force field is diagonal in the 3N dimensional space.

The cluster constituent intramolecular vibrational frequencies are considerably higher than those of the vdW modes. A reasonable approximation in this context then is to assume that the intramolecular modes are completely uncoupled from the low frequency vdW modes. Thus, the intramolecular modes are taken to be those of the cluster constituents. The constituent force fields are generated using the central force approximation[11] including out-of-plane motion terms. Since the vdW modes arise from the restriction of cluster constituent translations and rotations and the central force approximation adequately reproduces these degrees of freedom, the necessary uncoupling of the intramolecular modes and the intermolecular vdW modes is maintained along with providing adequate vdW mode calculational results. Other, more sophisticated force field approximations are tested in the calculations; the central force approximation is determined to be adequate for calculations of the vdW modes. The only restriction which applies is that the intramolecular field yields mode eigenvalues in the proper frequency regions.

Within the central force approximation, the force field contains only diagonal terms in the internuclear symmetry coordinate system. This diagonal force field provides a simple and convenient means of using approximate force constants for intramolecular motion in the calculations. The intramolecular force constants chosen are those pertaining to general functional group stretches and bends.[11]

The most convenient choice for a coordinate system as the working basis for matrix diagonalization is the Cartesian system. This coordinate

system is chosen since it is the system used in the present cluster configuration calculations, and more importantly, it is the coordinate system in which the $\underline{G}$ matrix is diagonal and obvious.

In order to combine the intermolecular and intramolecular force fields algebraically, the force fields are transformed into the Cartesian coordinate system. The transformation yields two 3N dimensional $\underline{F}$ matrices. The intramolecular matrix is designated as $\underline{F}_o$ and the intermolecular matrix is designated as $\underline{F}'$. The $\underline{F}_o$ matrix consists of two diagonal blocks containing the coordinates of cluster constituent intramolecular motion. The $\underline{F}'$ matrix contains two off-diagonal blocks and diagonal entries corresponding to the "perturbations" yielding the vdW motion. Adding these two matrices results in the "giant molecule" $\underline{F}$ matrix of order 3N. This matrix is left-multiplied by the $\underline{G}^{-1}$ matrix and numerically diagonalized with the eigenvalues and eigenvectors being determined in the usual fashion. Upon diagonalization, the eigenvalues and eigenvectors of intramolecular motion are identified along with those corresponding to cluster translation and rotation. These latter zero energy modes are discarded and the remaining modes are the eigenvalues and eigenvectors of the ground state vdW modes.

The intermolecular force constants used in the normal coordinate analysis are generated from the intermolecular vdW potential by making a harmonic approximation. Within this approximation, the force constant is simply the second derivative of the potential function,[9]

$$V(r_{ij}) = \sum_{i<j=1}^{n} \left[\left(\frac{A^{kl}}{r_{ij}^{12}} - \frac{C^{kl}}{r_{ij}^{6}} \right) (1 - \delta_{MP}^{ij}) + \frac{332.0\, q_i q_j}{D r_{ij}} + \left(\frac{A'^{kl}}{r_{ij}^{12}} - \frac{C'^{kl}}{r_{ij}^{6}} \right) \delta_{MP}^{ij} \right] + V(r_{ij})_{MP} + V(r_{ij})_{MQ} + V(r_{ij})_{MP} \quad (1)$$

The potential function contains a general nonbonded potential (NB), a monopole electrostatic potential (ME), and a general hydrogen bonded potential (HB) in a Lennard-Jones (6-12-1-10-12) form. The total intermolecular interaction is taken as a sum of pairwise atom-atom interactions over all the atoms of each cluster constituent. The r_{ij}'s are the atom-atom distances between atom i on constituent k and atom j on constituent l. The r_{ij}'s represent the symmetry coordinates in which the intermolecular force field is diagonal. The second derivative of eq. (1) with respect to r_{ij} gives the force constant of the atom-atom interaction as,

$$K_{ij}(r_{ij}) = \sum_{i=1}^{n}\sum_{j=1}^{m} \left[\left\{ \frac{12\cdot13\cdot A^{kl}}{r_{ij}^{14}} - \frac{6\cdot7\cdot C^{kl}}{r_{ij}^{8}} \right\} (1 - \delta_{HB}^{ij}) + \left\{ \frac{2\cdot332.0\, q_i q_j}{D\, r_{ij}^{3}} + \frac{12\cdot13\, A'^{kl}}{r_{ij}^{14}} - \frac{10\cdot11\cdot C'^{kl}}{r_{ij}^{12}} \right\} \delta_{HB}^{ij} \right] \qquad (2)$$

in which the K_{ij}'s are elements of the $\underline{F}'$ matrix expressed in intermolecular symmetry coordinates. These terms are evaluated at the equilibrium configuration of the cluster assuming that the cluster constituents are frozen with regard to intramolecular motion.

Three additional models are employed to study the benzene$(Ar)_1$ vdW cluster as a test case. In these models, the vdW cluster is assumed to be a "diatomic molecule" in the sense that the system is considered to be composed of two particles, the benzene molecule (solute) and the argon atom (solvent). The vdW modes are assumed to arise from restricted 1-dimensional motion of the benzene molecule relative to the argon atom. Only the atom-molecule benzene$(Ar)_1$ cluster will be considered using these models since its vdW modes are easily characterized by simple translations along any of the three Cartesian axes. The vdW stretching mode is taken as motion restricted to the

1-dimensional translation moving the cluster constituents apart in opposite directions. The vdW bending modes are considered to be motions restricted to 1-dimensional translations which move the cluster constituents parallel to one another in opposite directions.

In the first model considered, 1-dimensional potential curves are mapped out by translating the solvent molecule relative to the solute atom in one of the three Cartesian directions. The intermolecular vdW potential is assumed to be represented by a Taylor series expansion about the equilibrium intermolecular distance, R_o in the form,

$$U(R) = U(R_o) + \left(\frac{dU}{dR}\right)_{R=R_o} R + \frac{1}{2}\left(\frac{d^2U}{dR^2}\right)_{R=R_o} R^2 + \frac{1}{6}\left(\frac{d^3U}{dR^3}\right)_{R=R_o} R^3 + \frac{1}{24}\left(\frac{d^4U}{dR^4}\right)_{R=R_o} R^4 + \ldots \tag{3}$$

The expansion coefficients are evaluated by a polynomial fit to the potential curves taking the displacement vector R as the independent variable and U(R) as the dependent variable. The second-order polynomial fit coefficient determines the effective harmonic force constant governing the frequency of bound state motion. The energy of this motion is given by[12]

$$\omega_e = \frac{1}{2\pi C}\sqrt{\frac{k_{eff}}{\mu}}$$

$$\text{with} \quad k_{eff} = \left(\frac{d^2U}{dR^2}\right)_{R=R_o} = 2 \cdot (\text{second-order coefficent}), \tag{4}$$

$$\frac{1}{\mu} = \frac{1}{m_1} + \frac{1}{m_2},$$

and m_1 = solute mass

m_2 = solvent mass.

The third and fourth order polynomial fit coefficients represent an anharmonic correction term to the energy. From perturbation theory, the correction can be written to first order as[12]

$$\omega_e\chi_e = \frac{3h^2}{32\pi^4\omega_e^2\mu^2c^2}\left(\frac{5g^2h}{8\pi^2\omega_e^2\mu c} - j\right)$$

with g = (third-order coefficient) $= \frac{1}{6}\left(\frac{d^3U}{dR^3}\right)_{R=R_o}$ (5)

and j = (fourth-order coefficient) $= \frac{1}{24}\left(\frac{d^4U}{dR^4}\right)_{R=R_o}$

Higher order terms are neglected in the anharmonic corrections since $\omega_e >> \omega_e\chi_e >>$ other corrections. A polynomial least-squares fit to tenth order in R is determined to be sufficient to reproduce faithfully the 1-dimensional potential curves generated via translation. In passing we note that the Taylor series expansion could also be evaluated directly by taking successive derivatives of eq. (1). This may be the method of choice if one is only interested in the lowest order terms in evaluating eq. (4) or (5), or if one is interested in a more "exact" reproduction of the potential curves in the vicinity of the dissociation limit.

The second model considered involves fitting the 1-dimensional potential energy curves, derived in the same manner as previously discussed, to a Morse function of the form,[15]

$$U(R) = D_e(e^{-2f(R-R_o)} - 2e^{-f(R-R_o)}). \qquad (6)$$

The energy levels and anharmonic corrections are evaluated using

$$\omega_e = \beta \sqrt{\frac{D_e h}{2\pi^2 c\mu}} \qquad (7)$$

and

$$\omega_e \chi_e = \frac{\beta^2 h}{8\pi^2 c\mu} . \qquad (8)$$

The last model used involves an energy level fit based upon the semi-classical JWKB method.[13] In this model, the energy levels are determined from the quantization of the action integral according to the Bohr-Sommerfeld restrictions. The governing equation is

$$I = (2\mu)^{-\frac{1}{2}} \oint [E - U_{eff}(R)]^{\frac{1}{2}} \, dR = h(v + \tfrac{1}{2}). \qquad (9)$$

Energy level determination is accomplished by numerical integration of (9) taking $U_{eff}(R)$ as the 1-dimensional intermolecular vdW potential in a tenth order polynomial form. The path of integration is taken over one complete motion cycle with the boundary conditions established by the intermolecular potential at a specific energy E.

IV. Results.

A. Benzene$(Ar)_1$.

Figure 1 and Table I present the benzene$(Ar)_1$ vdW cluster spectrum recorded in the region between 38561 cm^{-1} and 38710 cm^{-1} using 1-color TOFMS. The cluster 6_o^1 is "red shifted" by 21 cm^{-1} with respect to the benzene 6_o^1. The bathychromic shift is indicative of the greater binding energy in the cluster S_1 state relative to the cluster S_o state. Three vibronic features are observed to the blue of the cluster 6_o^1. No features are observed in the symmetry "forbidden" benzene 0_o^o region; therefore, the cluster must have at least a three-fold axis of symmetry.

Figure 2 and Table II contain the calculational results of the ground state configuration and vdW modes of benzene$(Ar)_1$. Configurational calculations yield a single geometry of minimum energy for the cluster possessing C_{6v} symmetry, figure 2. In this geometry, the argon atom lies 3.44 Å above the benzene molecular plane along the z (6-fold) axis. The ground state cluster binding energy is calculated at 287 cm^{-1} which makes the excited state binding energy 308 cm^{-1}. The calculated intermolecular distance of 3.44 Å compares well with that of 3.4 Å obtained from the rotational analysis,[15] adding independent proof to the adequacy of the calculations in predicting detailed information on cluster structure.

The eigenvalue energies from the normal coordinate analysis of benzene$(Ar)_1$ are 40 cm^{-1} and 11 cm^{-1} for the vdW stretch and vdW bends, respectively. The eigenvector normal modes, figure 2, reveal that the vdW stretch entails purely perpendicular motion of the argon atom relative to the benzene molecular plane. Furthermore, the calculations reveal that the 2-fold degenerate vdW bending mode involves some combination of motion parallel to the benzene molecular plane. Both of these eigenvector results are consistent with group theoretical arguments as expected.

The "diatomic molecule" model calculations yield three sets of vdW mode energies. The average mode frequencies are 40 cm^{-1} for the vdW stretch, $s_z(a_1)$ and 10 cm^{-1} for the vdW bends $b_{xy}(e_1)$. Figures 3 and 4 show the details of the 1-dimensional potential curve mappings and the results of the model calculations. Note that the z-direction potential curve modeling the vdW stretch looks surprisingly similar in form to that of a typical diatomic molecule. All models yield both adequate potential curve fits and consistent vibrational energy level structures.

B. s-Tetrazine$(Ar)_1$.

Figure 5 presents the results of the ground state configuration and vdW mode analysis of s-tetrazine$(Ar)_1$. Only the normal coordinate analysis

vibrational calculation is presented since this method yields the most informative results for our purposes and the consistency between the eigenvalue/eigenvector results and the "diatomic molecule" results has already been shown for the benzene$(Ar)_1$ case. Configurational calculations yield a single cluster geometry of minimum energy possessing C_{2v} symmetry, figure 5. In this geometry, the argon atom lies 3.45 Å above the s-tetrazine molecular plane along the z (2-fold) axis. The calculated ground state cluster binding energy is 295 cm^{-1}. The calculated intermolecular distance of 3.45 Å compares extremely well with the intermolecular distance of 3.45 Å obtained from the rotational analysis. The calculated binding energy of 295 cm^{-1} also lies within the experimental limits of $254 < D_o'' < 332$ cm^{-1}.[5] Again, the calculations and experiment are in exact agreement.

The normal coordinate analysis eigenvalues are 41.0 cm^{-1} for the vdW stretching mode $s_z(a_1)$, 9 cm^{-1} for the vdW bending mode $b_y(b_1)$, and 12 cm^{-1} for the vdW bending mode $b_x(b_2)$. The eigenvector normal modes, figure 5, show that the vdW stretch is restricted to motion perpendicular to the s-tetrazine molecular plane while the vdW bends are restricted to motion parallel to the molecular plane. As in the benzene$(Ar)_1$ analysis, these results are consistent with group theoretical arguments.

C. Benzene$(CH_4)_1$.

The ground state configuration and vdW eigenvalues/eigenvectors for benzene$(CH_4)_1$ are shown in figure 6. The results presented for the geometry and binding energy of benzene$(CH_4)_1$ are in good agreement with previous reports from this laboratory using an exponential-six and Lennard-Jones potential form.[2] In this geometry, figure 6, the methane center-of-mass lies at 3.47 Å above the benzene molecular plane on the principle z (3-fold) axis. The cluster ground state binding energy is 540 cm^{-1}. The normal coordinate analysis reveals six vdW vibrations, two being 2-fold degenerate. The

ground state vibrational energies are 82 cm^{-1} for the vdW stretch $s_z(a_1)$, 16 cm^{-1} for the vdW bends $b_{xy}(e)$, and 28 cm^{-1} and 89 cm^{-1} for the vdW torsions $t_z(a_2)$ and $t_{xy}(e)$, respectively. The eigenvector normal modes, figure 6, transform as the translational and rotational representations of the C_{3v} point group, as indicated. The vdW stretching mode transforms as the translation of the cluster constituents away from one another along the z (3-fold) axis. The vdW bending modes transform as some combination of cluster constituent translations in opposite directions perpendicular to the 3-fold axis in the xy plane. One vdW torsion mode transforms as a rotation of the cluster constituents about the z (3-fold) axis in opposite directions. The remaining two vdW torsions transform as rotations about orthogonal axes perpendicular to the 3-fold axis.

D. Benzene$(H_2O)_1$.

The calculated benzene$(H_2O)_1$ geometry used in the normal coordinate analysis is similar to that calculated previously.[3] Only one minimum energy configuration, which has a binding energy of 504 cm^{-1}, is found. As shown in figure 7, the cluster geometry possesses C_s symmetry with the H_2O center-of-mass located 3.15 Å above the benzene molecular plane.

Six ground state vdW vibrations are calculated for the C_s cluster geometry. Their corresponding eigenvalues and eigenvectors are shown in figure 7. The six vdW modes consist of a vdW stretch at 159 cm^{-1}, two vdW bends at 14 cm^{-1} and 18 cm^{-1}, and three vdW torsions at 40 cm^{-1}, 50 cm^{-1}, and 156 cm^{-1}. The eigenvector normal modes transform as the translational and rotational representations of the C_s point group: the vdW stretch transforms as a z translation; the vdW bends transform as x and y translations; and the vdW torsions transform as R_x, R_y, and R_z rotations.

E. Benzene$(NH_3)_1$.

Configurational calculations on the benzene$(NH_3)_1$ cluster reveal two minimum energy geometries similar to those obtained previously.[3]

One cluster geometry possesses C_{3v} symmetry with a binding energy of 711 cm^{-1} while the other possesses C_s symmetry and a binding energy of 608 cm^{-1}. In the C_{3v} cluster, figure 8, the NH_3 center-of-mass is located 3.23 Å above the benzene molecular plane along the z (3-fold) axis. In the C_s cluster, figure 9, the NH_3 center-of-mass is located 3.29 Å above the benzene molecular plane.

Using the potential surfaces generated from these two configurations, six ground state vdW vibrations are calculated for each geometry. Their corresponding eigenvalues and eigenvectors are shown in figures 8 and 9. The C_{3v} cluster ground state normal modes transform in the same manner as those of benzene$(CH_4)_1$. In the C_s cluster, the ground state normal modes transform similar to those of benzene$(H_2O)_1$.

V. Discussion.

To compare the calculated and experimentally observed vdW modes, we assume that the intermolecular potential surface of the cluster is identical in both S_o and S_1 electronic states. This assumption is justifiable if one considers that cluster fluorescence excitation and dispersed emission spectra are similar for the vdW vibronic transitions.[4] Furthermore, the small spectral shifts of the chromophore and the weak intensity of the vdW modes signify only small changes in cluster binding energy. This is probably indicative of only slight variations of the potential surface between S_o and S_1 electronic states.

Comparisons between calculation and experiment are made using group theoretical arguments based on the selection rules governing the vibronic transitions. Specifically, transition moment matrix elements are qualitatively analyzed using the crude adiabatic approximation for which the vibrational mode dependence on the electronic wave function is explicit. In this case, a standard Herzberg-Teller (HT) expansion and adiabatic wave functions are used[14]

with the electronic wave function vibrational mode dependence truncated at second order.

Using this expansion, two unique types of spectra can be generated. First, one could consider that the vdW modes do not participate in the vibronic coupling scheme (Case I) and that they merely enter into the expansion as an additional scalar product (overlap integral). This argument dictates that only totally symmetric Franck-Condon progressions and combination bands are spectroscopically observed. Furthermore, the intensities of these features are solely derived from the cluster chromophore vibronic mode with which they are in combination. Alternately, one could consider the vdW modes to be capable of vibronic coupling (Case II). In this case, they enter into the HT transition moment equation in the same manner as other vibronically active modes. The operator responsible for these transitions would be of the form

$$\left(\frac{\partial^2 U}{\partial Q_6 \partial q_{vdw}}\right)_{Q_6 = Q_6^o,\ q_{vdw} = q_{vdw}^o} Q_6 q_{vdw}$$

in which Q_6 is the cluster ν_6 vibrational mode and q_{vdW} is a specific cluster vdW mode. This argument allows the possibility of observing nontotally symmetric vdW fundamentals with "borrowed" intensity due to interelectronic state mixing.

In the individual cluster discussions, the above two cases are considered in order to assign and understand the observed cluster vibronic spectra.

A. Benzene$(Ar)_1$.

Comparison of the calculated ground state vdW vibrations of benzene$(Ar)_1$ and the experimental vibronic spectrum, figure 1, Table I,

and Table II, shows that vibronic assignments can be made based upon calculations for all models analyzed. Considering the transition moment matrix elements for the benzene(Ar)$_1$ $S_1 \leftarrow S_0$ transition under C_{6v} symmetry, one should expect to observe totally symmetric combination bands of the vdW stretch built upon the cluster 6^1_0. The selection rule for these combination bands is $\Delta v = 0, \pm 1, \pm 2, \ldots$ Also, one should expect to observe nontotally symmetric vdW bend combinations with the 6^1_0 with the selection rule being $\Delta v = 0, \pm 2, \pm 4 \ldots$ These selection rules hold for both Case I and Case II type spectra and imply that the vdW modes do not enter into the vibronic intensity borrowing mechanism.

The calculated vdW stretching mode at 40 cm^{-1} compares quite well with the experimental vibronic feature at 39.7 cm^{-1} to the blue of the benzene(Ar)$_1$ 6^1_0. Thus, this feature is assigned to the benzene(Ar)$_1$ vdW stretch/cluster 6^1_0 combination band $6^1_0\, s_z(a_1)^1_0$ based upon the $\Delta v = 0, \pm 1, \pm 2 \ldots$ selection rule.

For the vdW bending modes, only odd overtones are expected to be observed as pointed out above. The experimentally observed features at 30.9 cm^{-1} and 61.8 cm^{-1} to the blue of the cluster 6^1_0 correspond to overtone features of the vdW bends; using the $\Delta v = 0, \pm 2, \pm 4 \ldots$ selection rule, the former feature is the first overtone of the vdW bends and the latter is the third. Considering the 30.9 cm^{-1} feature as the first overtone places the symmetry forbidden bend fundamental at about 15.5 cm^{-1}. This energy lies close to the calculated 2-fold degenerate ground state vdW bend at 11 cm^{-1}. Thus, these two spectral features are assigned to the benzene(Ar)$_1$ vdW bends first and third overtone/cluster 6^1_0 combination bands, $6^1_0\, b_{xy}(e_1)^2_0$ and $6^1_0\, b_{xy}(e_1)^4_0$.

Ramifications of Herzberg-Teller vibronic coupling in the benzene(Ar)$_1$ cluster are obvious. From the derived vibronic selection rules and experi-

mental observation, the benzene$(Ar)_1$ cluster spectrum is best assigned based upon benzene Herzberg-Teller coupling (i.e., the 6^1_0 feature is allowed) with vdW totally symmetric modes and combinations forming short, weak Franck-Condon progressions built upon the intense benzene transition. In addition, the calculated and observed[15] C_{6v} cluster symmetry is verified by the vdW vibronic structure.

B. s-Tetrazine$(Ar)_1$.

The selection rules governing the s-tetrazine$(Ar)_1$ vdW vibronic transitions under C_{2v} symmetry arise from Case I Franck-Condon arguments. The totally symmetric vdW stretch should be observed to the blue of the cluster 0^o_o following a $\Delta v = 0, \pm1, \pm2, \ldots$ selection rule. The vdW bends should only be observed in odd overtones ($\Delta v = 0, \pm2, \pm4 \ldots$) built on the allowed s-tetrazine 0^o_o transition. As in the benzene$(Ar)_1$ cluster, no Case II distinction can be made for s-tetrazine$(Ar)_1$ and thus no vdW Herzberg-Teller vibronic coupling is expected. Unfortunately, a complete experimental spectrum showing the details of the s-tetrazine$(Ar)_1$ vdW modes is not, as yet, available. The only information in this regard is the identification of the vdW stretching mode at 44 cm^{-1} to the blue of the cluster 0^o_o by Levy et al.[5] Other vdW features at 66 cm^{-1} and 108 cm^{-1} to the blue of the cluster 0^o_o are observed, but they are neither assigned nor are their spectra published.

Figure 10 and Table III compare the calculated ground state vdW mode frequencies with those observed in the s-tetrazine$(Ar)_1$ $^1B_{3u} \leftarrow {}^1A_g$ vdW vibronic spectrum. The experimentally assigned vdW stretch at 44 cm^{-1} to the blue of the cluster 0^o_o corresponds to the 41 cm^{-1} calculated ground state stretch. This motion, like that in the benzene$(Ar)_1$ cluster, involves perpendicular motion of the argon atom relative to the s-tetrazine molecular

plane. Based upon ground state calculations, the feature 66 cm^{-1} to the blue of the cluster 0_o^o probably corresponds to a vdW stretch/vdW bend overtone combination band, $s_z(a_1)_o^1\ b_x(b_2)_o^2$ or $s(a_1)_o^1\ b_y(b_1)_o^2$; the feature at 108 cm^{-1} probably corresponds to the next allowed bend overtone/stretch combination band $s(a_1)_o^1\ b_x(b_2)_0^4$ or $s(a_1)_o^1\ b_y(b_1)_o^4$. No speculation with regard to which bend is responsible for the features observed will be made since no spectra of sufficient sensitivity are available for analysis.

C. Benzene$(CH_4)_1$

In a previous analysis of the benzene$(CH_4)_1$ cluster,[2] three major vdW vibronic features were reported in the cluster 6_o^1 region: these features were assigned to a bend fundamental (27.3 cm^{-1}), a stretch fundamental (32.3 cm^{-1}), and a stretch overtone (51.4 cm^{-1}). The assignments were made based upon the assumptions described in the Introduction.

Considering the HT transition moment matrix elements and assuming a Case I type spectrum, the selection rules for the benzene$(CH_4)_1$ vdW vibronic transitions are $\Delta v = 0, \pm1, \pm2, \ldots$ for the vdW stretch and $\Delta v = 0, \pm2, \pm4, \ldots$ for the vdW bends and torsions when in combination with the cluster 6_o^1.

The selection rules involved in Case II can be viewed in two ways. The selection rules can be derived using the calculated cluster symmetry of C_{3v}, or they can be derived by considering the cluster symmetry as C_{6v}. The latter situation arises since the methane center-of-mass is calculated at 3.47 Å above the benzene molecular plane. At this distance, the methane could be viewed as a sphere above the benzene molecular plane and, hence, the use of the C_{6v} point group to represent the vdW mode symmetries could be warranted.

In C_{3v} symmetry Case II, the selection rules for vdW mode combinations with the cluster 6_o^1 are $\Delta v = 0, \pm1, \pm2, \ldots$ for all six vdW modes. If C_{3v} is the correct cluster physical symmetry and HT vdW coupling exists, all modes can be observed in the cluster 6_o^1 region. In C_{6v} symmetry, Case II, the selec-

tion rules for the vdW mode combinations with the cluster 6^1_o are $\Delta v = 0, \pm1, \pm2, \ldots$ for the vdW stretch $s_z(a_1)$ and torsion $t_z(a_2)$ and $\Delta v = 0, \pm2, \pm4, \ldots$ for the 2-fold degenerate vdW bends $b_{xy}(e_1)$ and torsions $t_{xy}(e_1)$. In this approximate high symmetry, only the cluster 6^1 and vdW mode t_z are capable of vibronic coupling for the 6^1_o transition.

Comparison of the experimental 6^1_o vibronic spectrum of benzene$(CH_4)_1$ and the calculated ground state vdW vibrations is shown in figure 12 and Table IV. The observed feature at 27.3 cm^{-1} to the blue of the cluster 6^1_o corresponds to the t_z torsion calculated at 28 cm^{-1}. Thus, this feature and its observed overtones at 51.4 cm^{-1} and 73.5 cm^{-1} are reassigned to 6^1_o vdW torsion combination bands $6^1_o\ t_z(a_2)^1_o$, $6^1_o\ t_z(a_2)^2_o$, and $6^1_o\ t_z(a_2)^3_o$, using the C_{3v} Case II or C_{6v} Case II $\Delta v = 0, \pm1, \pm2, \ldots$ selection rule. The $\Delta v = 0, \pm1, \pm2, \ldots$ selection rule suggests that for the benzene$(CH_4)_1$ system vdW mode Herzberg-Teller vibronic coupling is an important component of the overall intensity mechanism. In the present case, the occurrence of the nontotally symmetric t_z torsion progression implies that the vdW modes are vibronically active and that assuming them to be nonparticipants in the coupling mechanism oversimplifies the physics necessary to explain the cluster's spectroscopy.

The intense feature at 32.3 cm^{-1} to the blue of the cluster 6^1_o corresponds to the first overtone of the 2-fold degenerate vdW bending mode, $6^1_o\ b_{xy}(e)^2_o$, calculated at 16 cm^{-1}. This identification is based upon the observation of a feature at 64.6 cm^{-1} which corresponds to the third overtone of the bends. Furthermore, weak intensity features are observed at about 16.1 cm^{-1} and 48.4 cm^{-1} which could correspond to the vdW bend fundamentals and second overtones. The observation of these features adds proof to the arguments suggesting that the vdW modes are, at least, minor participants in the Herzberg-Teller vibronic coupling scheme. The cluster symmetry and, hence, spectroscopy are thereby also best described using the calculated C_{3v} point group in con-

junction with Herzberg-Teller coupling rather than the approximate C_{6v} point group. Based upon this, the features at 32.3 cm^{-1} and 64.6 cm^{-1} are reassigned to vdW bend overtone combinations with the cluster 6_o^1; $6_o^1\, b_{xy}(e)_o^2$ and $6_o^1\, b_{xy}(e)_o^4$ using the C_{3v} selection rule $\Delta v = 0, \pm1, \pm2, \ldots$. The features are assigned in Table IV and figure 11. The weak features at 16.1 cm^{-1} and 48.4 cm^{-1} are assigned to $6_o^1\, b_{xy}(e)_o^1$ and $6_o^1\, b_{xy}(e)_o^3$. Based upon the relative intensities displayed in the spectrum, vdW vibronic coupling is an important factor in the intensity of this progression involving the e symmetry bending modes.

Neither the vdW stretch $s_z(a_1)$ nor the 2-fold degenerate torsions $t_{xy}(e)$ are observed in the 6_o^1 spectrum. This could be due to poor Franck-Condon factors for these vibronic transitions since they are both calculated to be at relatively high energies (ca. 82 cm^{-1} and 89 cm^{-1}, respectively). Moreover, these modes could be participating in VP since the total energy $6_o^1\, s_z(a_1)_o^1$ or $6_o^1 t_{xy}(e)_o^1$ is close to that of, if not above, the cluster's S_1 binding energy. Both the vdW stretch and t_{xy} torsions involve motion perpendicular to the benzene molecular plane: this motion could couple well to the VP process.

D. Benzene$(H_2O)_1$.

The $S_1 \leftarrow S_o$ vibronic spectrum of benzene$(H_2O)_1$ previously observed in this laboratory[3] possesses two unique spectral regions located around the cluster 0_o^o and 6_o^1 containing vdW vibronic features. No vdW vibronic assignments were made in either region and no correlation between the regions was suggested.

Examination of the HT transition moment matrix elements using C_s symmetry and Case I considerations leads to the selection rules $\Delta v = 0, \pm1, \pm2, \ldots$ for the vdW s_z stretch, b_y bend, and t_x torsion and $\Delta v = 0, \pm2, \pm4, \ldots$ for the b_x bend, t_y and t_z torsions. Under Case II arguments, the selection rule is $\Delta v = 0, \pm1, \pm2, \ldots$ for all six vdW modes: all modes are capable of vibronic coupling.

Vibronic spectra of benzene$(H_2O)_1$ in both the cluster 0_o^o and 6_o^1 regions are reproduced in figure 12 along with the calculated ground state vdW mode energies. The observed feature at 5.2 cm^{-1} (4.8 cm^{-1}) to the blue of the cluster 0_o^o (6_o^1) transition corresponds to the vdW b_x bend fundamental calculated at 14 cm^{-1}. The observed feature at 16.2 cm^{-1} (15.8 cm^{-1}) to the blue of the cluster 0_o^o (6_o^1) transition corresponds to the calculated totally symmetric vdW b_y bend at 18 cm^{-1}. Additionally, the observed features at 34.6 cm^{-1} (34.6 cm^{-1}) and 49 cm^{-1} (48.4 cm^{-1}) to the blue of the cluster 0_o^o (6_o^1) transition are associated with the $t_z(a'')$ and $t_x(a')$ torsion fundamentals calculated at 40 cm^{-1} and 50 cm^{-1}, respectively. The occurrence of the nontotally symmetric fundamentals implies that the $\Delta v = 0, \pm 2, \pm 4, \ldots$ selection rule for Case I in which the vdW modes are not vibronically coupled is violated. The violation suggests that the vdW modes participate in the vibronic coupling scheme and that the $\Delta v = 0, \pm 1, \pm 2, \ldots$ selection rule should apply to all six vdW modes (Case II). Based upon this, the spectra are best assigned, Table V and figure 12, using both nontotally and totally symmetric vdW progressions.

Assigning the benzene$(H_2O)_1$ spectra using the C_s point group representations corroborates the calculated cluster geometry. Treating the cluster in approximate high symmetries, such as C_{2v}, leads to selection rules which are clearly violated when applied to spectral observation and assignment. Specifically, the bend and torsion fundamentals are forbidden under these higher symmetry approximations. Furthermore, the spectral assignments using C_s symmetry arguments suggest that the water constituent is likely located above the benzene molecular plane.

Neither the vdW s_z stretch nor the t_y torsion are observed in either spectral region. This, as in the benzene$(CH_4)_1$ case, probably results from poor Franck-Condon factors for these particular modes; they are both

calculated to be at relatively high energies (ca. 159 cm^{-1} and 156 cm^{-1}, respectively). Moreover, in the 6_0^1 region, these modes could be participating in VP since the total energy of the system at these levels is close to, if not above, the cluster binding energy (c.a. = 500 cm^{-1}). The decrease in the hypsochromic shift and the shift of intensity maximum in the vdW manifold in going from the cluster 0_0^0 to the 6_0^1 may also be indicative of a VP process.

E. Benzene$(NH_3)_1$.

Benzene$(NH_3)_1$ clusters recently observed in this laboratory[3] yield spectra in both the cluster 0_0^0 and 6_0^1 regions. Two cluster geometries are calculated for the system, one possessing C_s symmetry and the other possessing C_{3v} symmetry. From symmetry arguments the C_s symmetry cluster is the only contributor to the 0_0^0 spectrum while both cluster geometries contribute to the 6_0^1 spectrum. Neither of these spectra were analyzed nor assigned in the initial observation since they are so complicated. They were merely presented as an indication of the notion that cluster vibronic spectra can sometimes be very extensive and congested.

The benzene$(NH_3)_1$ C_s symmetry cluster follows the same vdW vibronic selection rules as derived for the benzene$(H_2O)_1$ cluster. In this symmetry, the selection rules for Case I are $\Delta v = 0, \pm1, \pm2, \ldots$ for the vdW stretch, b_y bend, and t_x torsion and $\Delta v = 0, \pm2, \pm4, \ldots$ for the b_x bend, t_y and t_z torsions. In Case II the selection rule is $\Delta v = 0, \pm1, \pm2, \ldots$ for all six vdW modes. Furthermore, the calculated cluster geometries are qualitatively similar. Hence, their 0_0^0 spectra should be qualitatively similar: this is borne out in both experimental results and vibrational mode calculations.

The benzene$(NH_3)_1$ C_{3v} symmetry cluster follows the same vibronic selection rules as presented for benzene$(CH_4)_1$. Here the selection rules are either $\Delta v = 0, \pm1, \pm2, \ldots$ for the vdW stretch and $\Delta v = 0, \pm2, \pm4, \ldots$ for the vdW bends and torsions (Case I) or $\Delta v = 0, \pm1, \pm2, \ldots$ for all six vdW modes (Case II).

The calculated ground state vibrational energies and the observed cluster 0_o^o and 6_o^1 vibronic spectra are compared in figure 13. Due to the complex nature of the spectra which possibly results from hindered NH_3 rotation within the cluster and hot bands, only tentative assignments of the vdW mode progressions are made. The tentative assignments are based upon both vibrational mode calculations and upon inference from the benzene$(H_2O)_1$ and benzene$(CH_4)_1$ cluster spectra.

In the 0_o^o spectrum, the most intense low energy feature is assigned to the origin of the cluster's $S_1 \leftarrow S_o$ transition. The smaller intensity features to the red of this feature are thus hot bands which yield the sequence structure in the 0_o^o region. The observed feature at 8.8 cm^{-1} to the blue of the cluster 0_o^o corresponds to the nontotally symmetric vdW b_x bend fundamental calculated at 15 cm^{-1}. Additionally, the observed features at 15.0 cm^{-1}, 45.1 cm^{-1}, 54.2 cm^{-1}, 99.6 cm^{-1}, and 127.7 cm^{-1} correspond to the calculated b_y bend (21 cm^{-1}), t_z torsion (44 cm^{-1}), t_x torsion (48 cm^{-1}), stretch (112 cm^{-1}), and t_y torsion (125 cm^{-1}). The occurrence of the nontotally symmetric fundamentals suggests that the vdW modes participate in vibronic coupling (Case II) and that the $\Delta v = 0, \pm 1, \pm 2, \ldots$ selection rule should apply to all six vdW modes. Using this selection rule, the spectrum is best assigned, Table VI, using both nontotally and totally symmetric vdW progressions.

In the 6_o^1 spectrum, the most intense low energy feature is assigned to the cluster 6_o^1 vibronic origin. This assignment bears a resemblance to the benzene$(H_2O)_1$ 6_o^1 spectrum in the respect that the 6_o^1 features for both clusters are red shifted relative to that observed at the $S_1 \leftarrow S_o$ origins (ca. 25 cm^{-1} for benzene$(NH_3)_1$ and 35 cm^{-1} for benzene$(H_2O)_1$).

Table VI presents the C_s symmetry geometry assignments in the 6_o^1 region. The assignments are made using the vdW fundamentals identified in the 0_o^o spectrum and $\Delta v = \pm 1, \pm 2, \ldots$ selection rule for all six vdW modes (Case II).

The contribution of the C_{3v} symmetry benzene$(NH_3)_1$ cluster to the 6_o^1 spectrum is observed starting with the feature at 72.9 cm^{-1} to the blue of the C_s cluster 6_o^1. Assignment of this feature to the C_{3v} cluster 6_o^1 is based upon the observation that no intense features are seen in either the benzene$(NH_3)_1$ 0_o^o or the benzene$(H_2O)_1$ 6_o^1 spectra at this energy. The observed feature at 15 cm^{-1} to the blue of the C_{3v} cluster 6_o^1 corresponds to the 2-fold degenerate vdW b_{xy} bends at 19 cm^{-1}. The observed feature at 53 cm^{-1} to the blue of the C_{3v} cluster 6_o^1 is associated with the calculated t_z torsion at 44 cm^{-1}. As in the benzene$(CH_4)_1$ case, the observation of the b_{xy} and t_z fundamentals implies that the vdW modes participate in the vibronic coupling mechanism (Case II) and that the $\Delta v = \pm 1, \pm 2, \ldots$ vibronic selection rule applies for all vdW modes. Based upon this, the best assignments for the C_{3v} cluster vdW vibronics are tabulated in Table VI.

F. Morse $\frac{6}{R_o}$ Model.

Calculations of the ground state vdW modes of benzene$(Ar)_1$ are also conducted using a model described by Jortner et al.[1,6,7] This model contains a main feature which, at first glance, appears to make it generally applicable in predicting vdW stretching mode frequencies from calculated cluster binding energies and equilibrium intermolecular distances. However, the model turns out to be incorrect in this application. The model employs a simple relationship between the cluster equilibrium intermolecular distance R_o and the Morse potential parameter β. The relation is derived by equating the second derivative of eq. (6) with the second derivative of a single term (6-12) potential function. This derivation yields the relation $\beta = \frac{6}{R_o}$ which can be used to predict the vdW stretching mode frequency by diatomic Morse fit methods.

Substituting $\beta = \frac{6}{R_o}$ and the calculated ground state cluster binding energy into eq. (7) yields a vdW stretching mode energy of 47 cm^{-1} for benzene$(Ar)_1$ employing Scheraga's potential parameters. Even though the calculated vibrational energy is qualitatively correct, figures 14 and 3 show that the $\beta = \frac{6}{R_o}$ relation results in an inadequate reproduction of the potential curve, especially in the critical region near the equilibrium intermolecular distance. Additional calculations using the potential data described in ref. 1 and the above approximate model also result in an inadequate potential curve reproduction, figure 15. In this case, the vdW stretching mode is calculated at 55 cm^{-1}.

The failure of the model under both data sets suggests that the model itself is inadequate in this application. The model fails in this application since the $\beta = \frac{6}{R_o}$ relation holds exactly only in systems in which the molecule-atom Lennard-Jones parameters have been determined directly. Applying this approximate model to a case in which the potential function is represented by pairwise atom-atom potentials does not take into account the differing contributions of each interaction to the potential energy and the equilibrium intermolecular distance. In this more complicated situation, no analytic relationship between β and R_o exists.

Comparing the vdW stretching mode energies calculated using Jortner's and Scheraga's data sets suggests that a significant difference exists between the two data sets. Benzene$(Ar)_1$ configurational calculations using Jortner's data set yield a single cluster geometry of C_{6v} symmetry with the argon atom located 3.5 Å above the benzene molecular plane. In this case, the ground state cluster binding energy is 395 cm^{-1}. This binding energy is 108 cm^{-1} greater than that calculated using Scheraga's data set. The binding energy of 287 cm^{-1} calculated using Scheraga's data set is probably more accurate since the benzene$(Ar)_1$ ground state binding energy should be very similar to that cal-

culated for s-tetrazine$(Ar)_1$. In the latter case, the calculated ground state binding energy of 295 cm^{-1} compares well with that observed experimentally, $254 < D_o'' < 332$ cm^{-1}.[5] Furthermore, generating Lennard-Jones parameters using the data set of ref. 1 yields a binding energy of 359 cm^{-1} for s-tetrazine$(Ar)_1$ which is clearly not as accurate as the binding energy reported in this work. The difficulty is due to the consolidation of atom-atom parameters from different data sets. In this respect, great caution must be taken when consolidating parameters since each parameter set is, in general, only self-consistent and may have no meaning when combined with parameters from other sets.

VI. Conclusions.

TOFMS studies have been employed to determine the general geometry and symmetry of vdW clusters in the gas phase. Through computer modeling, a correlation between the details of the cluster geometry and spectral features has been demonstrated. Specifically, the parametric calculations yield useful information regarding cluster geometry, binding energy, and the vdW vibrations. These calculated results are consistent with experiment and serve as predictive and analytic tool which can be used to elucidate and understand the details of vdW cluster energetics.

Of the several models considered in studying the intermolecular vdW modes, simple diatomic approximations yield adequate results when applied to atom-molecule clusters. On the other hand, for molecule-molecule clusters normal coordinate analysis is essential. The normal coordinate analysis is especially useful for analyzing systems which have little or no symmetry since no a priori knowledge of vdW mode nature is necessary to generate potential energy surface mappings.

Reassignments of and assignments to cluster vdW modes have been made based upon the knowledge gained from calculation. From comparison of

calculation and experiment, several conclusions result. First, the actual excited state normal mode vdW frequencies are well fit by the calculated ground state cluster potential. This conclusion, though not surprising, gives independent proof of the invariance of the weak vdW potential between ground and excited electronic states as well as providing a means of using ground state vdW vibrational structure to predict vdW vibronic structure. Second, in the majority of the clusters analyzed, the observed vdW vibrations are those involving bending and torsional motions parallel to the aromatic π-system. Furthermore, these modes are, in general, quite active in the Herzberg-Teller vibronic coupling mechanism and significant interelectronic state mixing obtains. Third, vdW motions which penetrate the aromatic π-system have high frequencies and are only observed in systems in which the Franck-Condon factors and binding energies are favorable. Finally, the observed vibronic structure supports the calculated cluster geometry in all cases.

Acknowledgement

We wish to thank Professor W. Klemperer for a number of helpful, informative, and stimulating discussions concerning van der Waals molecules and the nature of their vibrational spectra.

REFERENCES

1. M.J. Ondrechem, Z. Berkovitch-Yellin, and J. Jortner, J. Amer. Chem. Soc. 103, 6586 (1981).

2. M. Schauer and E.R. Bernstein, J. Chem. Phys. 82, 726 (1985).

3. J. Wanna, J.A. Menapace and E.R. Bernstein, J. Chem. Phys. to be published.

4. T.A. Stephenson and S.A. Rice, J. Chem. Phys. 81, 1083 (1984).

5. D.V. Brumbaugh, J.E. Kenny, and D.H. Levy, J. Chem. Phys. 78, 3415 (1983).

6. M.L. Sage and J. Jortner, J. Chem. Phys. 82, 5437 (1985).

7. J.A. Beswick and J. Jortner, J. Chem. Phys. 68, 2277 (1978); 69, 512 (1978); 74, 6725 (1981); 71, 4737 (1979).

8. J. Wanna and E.R. Bernstein, J. Chem. Phys. 84 927 (1986), and ref. 2 and 3, for example.

9. F.A. Momany, L.M. Carruthers, R.F. McGuire, and H.A. Scheraga, J. Phys. Chem. 78, 1595 (1974); G. Nemethy, M.S. Pottle, and H.A. Scheraga, J. Phys, Chem. 87 1883 (1983).

10. E.B. Wilson Jr., J.C. Decius, and P.C. Cross, "Molecular Vibrations, Theory of Infrared and Raman Vibrational Spectra", (McGraw-Hill Book Co., Inc., 1955).

11. G. Herzberg, "Molecular Spectra and Molecular Structure: II Infrared and Raman Spectra of Polyatomic Molecules", (Van Nostrand Reinhold Co, 1945).

12. G. Herzberg, "Molecular Spectra and Molecular Structure: I Spectra of Diatomic Molecules", (Van Nostrand Reinhold Co, 1950).

13. J.I. Steinfield, "Molecules and Radiation: An Introduction to Modern Molecular Spectroscopy", (MIT Press, 1978).

14. G. Fischer, "Vibronic Coupling: The Interaction Between Electronic and Nuclear Motions", (Academic Press, 1984).

15. K.H. Fung, H.L. Selzle, and E.W. Schlag, Z. Naturforsch, 36A, 1338 (1981).

TABLE I

vdW spectral features in benzene$(Ar)_1$ 6^1_o region and calculated ground state vdW modes (refer to fig. 1).

Energy Relative to Cluster 6^1_o (cm^{-1})	Calculated Ground State Energy (cm^{-1}) [a]	Assignment [a]
0 (38587.6)		6^1_o
	11 (b_{xy})	
30.9		$6^1_o b_{xyo}^2$
39.7	40 (s_z)	$6^1_o s_{zo}^1$
61.8		$6^1_o b_{xyo}^4$

a) vdW mode representations as per fig. 2.

TABLE II

Calculated ground state vdW mode energies for benzene$(Ar)_1$.

Model	s_z (cm^{-1}) [a]	b_{xy} (cm^{-1}) [a]
Taylor Series	40.88 (1.51)	9.80 (.03)
Morse Fit	39.47 (1.36)	10.54 (.10)
JWKB	40.05 (1.43)	9.71 (.02)
Normal Coordinate Analysis	40.0	11.0

a) Values in parentheses are first order anharmonicity corrections calculated from "diatomic molecule" models. vdW mode representations as per fig. 2.

TABLE III

vdW spectral features in s-tetrazine(Ar)$_1$ 0_o^o region (s-tetrazine $^1B_{3u} \leftarrow {}^1A_g$) and calculated ground state vdW modes (refer to fig. 10).

Energy Relative to Cluster 0_o^o (cm^{-1}) [c]	Calculated Ground State Energy (cm^{-1}) [b]	Assignment [b]
0 (18104.9)		0_o^o
	9 (b_y)	
	12 (b_x)	
44 [a]	41 (s_z)	s_{zo}^1
66		$s_{zo}^1 b_{xo}^2$ or $s_{zo}^1 b_{yo}^2$
108		$s_{zo}^1 b_{xo}^4$ or $s_{zo}^1 b_{yo}^4$

a) Observed and assigned in ref. 5.

b) vdW mode representations as per fig. 5.

c) From ref. 5.

TABLE IV

vdW spectral features in benzene$(CH_4)_1$ 6_o^1 region and calculated ground state vdW modes (refer to fig. 11).

Energy Relative to Cluster 6_o^1 (cm^{-1}) [a]	Calculated Ground State Energy (cm^{-1}) [b]	Assignment [b]
0 (38567.6)		6_o^1
16.1	16 (b_{xy})	$6_o^1 b_{xyo}^1$
27.3	28 (t_z)	$6_o^1 t_{zo}^1$
32.3		$6_o^1 b_{xyo}^2$
48.4		$6_o^1 b_{xyo}^3$
51.4		$6_o^1 t_{zo}^2$
64.6		$6_o^1 b_{xyo}^4$
73.5		$6_o^1 t_{zo}^3$
	82 (s_z)	
	89 (t_{xy})	

a) From ref. 2 and unpublished spectra.

b) vdW mode representations as per fig. 6.

TABLE V

vdW spectral features in benzene$(H_2O)_1$ 0_o^o and 6_o^1 regions and calculated ground state vdW modes (refer to fig. 12).

Energy Relative to Cluster 0_o^o (cm^{-1}) or 6_o^1 (cm^{-1}) [a]	Calculated Ground State Energy (cm^{-1}) [b]	Assignment [b]
0 (38168.6)		0_o^o
5.2	14 (b_x)	b_{xo}^1
16.2	18 (b_y)	b_{yo}^1
21.4		$b_{xo}^1 b_{yo}^1$
25		$b_{xo}^2 b_{yo}^1$
31.9		b_{yo}^2
34.6	40 (t_z)	t_{zo}^1
39.4		$t_{zo}^1 b_{xo}^1$
45.7		b_{yo}^3
49	50 (t_x)	t_{yo}^1
50.8		$t_{zo}^1 b_{yo}^1$
67.4		$t_{yo}^1 b_{yo}^1$
70.3		t_{zo}^2
99.5		t_{yo}^2
103.5		t_{zo}^3
-	156 (t_y)	
-	159 (s_z)	
0 (38655.4)		6_o^1
4.8	14 (b_x)	$6_o^1 b_{xo}^1$

TABLE V (Continued)

15.8	18 (b_y)	$6^1_o b_{yo}^1$
25.5		$6^1_o b_{xo}^2 b_{yo}^1$
30.3		$6^1_o b_{yo}^2$
34.6	40 (t_z)	$6^1_o t_{zo}^1$
39.6		$6^1_o t_{zo}^1 b_{xo}^1$
48.4	50 (t_x)	$6^1_o t_{yo}^1$
60.5		$6^1_o b_{yo}^4$
97.8		$6^1_o t_{yo}^2$
101.0		$6^1_o t_{zo}^3$
	156 (t_y)	
	159 (s_z)	

a) From ref. 3.

b) vdW mode representations as per fig. 7.

TABLE VI

vdW spectral features in benzene$(NH_3)_1$ 0_0^0 and 6_0^1 regions and calculated ground state vdW modes (refer to fig. 13).

Energy Relative to [a] Cluster 0_0^0 or 6_0^1 (cm^{-1})	Calculated Ground State Energy (cm^{-1}) [b]	Assignment [b c]
-39.2		b_{y2}^0
-36.7		
-33.4		$b_{x2}^0 b_{y1}^0$
-31.3		$b_{y2}^0 b_{xo}^1$
-29.6		
-26.7		$b_{x1}^0 b_{y1}^0$
-19.2		b_{y1}^0
- 6.7		b_{x1}^0
- 3.8		
0 (38021.1)		0_0^0
8.8	15 (b_x)	b_{xo}^1
15.0	21 (b_y)	b_{yo}^1
17.9		b_{xo}^2
24.2		$b_{xo}^1 b_{yo}^1$
26.7		b_{xo}^3
29.2		b_{yo}^2
32.1		$b_{xo}^2 b_{yo}^1$
34.2		b_{xo}^4
37.6		$b_{xo}^1 b_{yo}^2$
41.7		
45.1	44 (t_z)	t_{zo}^1
50.9		
54.2	48 (t_x)	t_{xo}^1

TABLE VI (Continued)

59.7		$t_{zo}^{1}b_{yo}^{1}$
64.7		$t_{xo}^{1}b_{xo}^{1}$
70.4		$t_{xo}^{1}b_{yo}^{1}$
75.5		$t_{xo}^{1}b_{xo}^{2}$
77.2		
80.1		$t_{xo}^{1}b_{xo}^{1}b_{yo}^{1}$
83.8		$t_{xo}^{1}b_{yo}^{2}$
99.6	112 (s_z)	s_{zo}^{1}
101.8		$t_{xo}^{1}t_{zo}^{1}$
107.2		$s_{zo}^{1}t_{xo}^{1}$
111.8		$t_{xo}^{1}t_{zo}^{1}b_{xo}^{1}$
114.3		$s_{zo}^{1}b_{yo}^{1}$
119.3		$t_{xo}^{1}t_{zo}^{1}b_{xo}^{2}$
122.7		$s_{zo}^{1}b_{xo}^{1}b_{yo}^{1}$
127.7	125 (t_y)	t_{yo}^{1}
- 9.0		$6_{o}^{1}b_{x1}^{o}$
- 4.9		
- 2.0		
0 (38514.7)		$6_{o}^{1}(C_s)$
2.0		
9.0	15 (b_x)	$6_{o}^{1}b_{xo}^{1}$
13.1	21 (b_y)	$6_{o}^{1}b_{yo}^{1}$
22.1		
26.2		$6_{o}^{1}b_{xo}^{3}$
29.5		$6_{o}^{1}b_{yo}^{2}$
32.0		$6_{o}^{1}b_{xo}^{2}b_{yo}^{1}$
34.4		$6_{o}^{1}b_{xo}^{4}$
37.3		$6_{o}^{1}b_{yo}^{2}b_{xo}^{1}$

TABLE VI (Continued)

45.1	44 (t_z)	$6_o^1 t_{zo}^1$
48.7		
53.7		$6_o^1 t_{zo}^1 b_{xo}^1$
55.3	48 (t_x)	$6_o^1 t_{xo}^1$
58.6		$6_o^1 t_{zo}^1 b_{yo}^1$
61.0		$6_o^1 t_{zo}^1 b_{xo}^2$
64.7		$6_o^1 t_{xo}^1 b_{xo}^1$
68.8		$6_o^1 t_{xo}^1 b_{yo}^1$
72.9 [0 (38587.6)]		$6_o^1(C_{3v})$
74.6		$6_o^1 t_{xo}^1 b_{xo}^2$
79.5		$6_o^1 t_{xo}^1 b_{xo}^1 b_{yo}^1$
83.3		$6_o^1 t_{xo}^1 b_{yo}^2$
87.9	19 (b_{xy})	$6_o^1 b_{xyo}^1(C_{3v}$
98.7	112 (s_z)	$6_o^1 s_{zo}^1$
100.4		$6_o^1 t_{xo}^1 t_{zo}^1$
103.9		$6_o^1 b_{xyo}^2(C_{3v})$
107.1		$6_o^1 s_{zo}^1 b_{xo}^1$
111.9		$6_o^1 t_{xo}^1 t_{zo}^1 b_{xo}^1$
114.0		$6_o^1 s_{zo}^1 b_{yo}^1$
123.4		$6_o^1 s_{zo}^1 b_{xo}^1 b_{yo}^1$
125.9	44 (t_z)	$6_o^1 t_{zo}^1(C_{3v})$
-	97 (s_z)	-
-	152 (t_{xy})	-

a) From ref. 3.

b) vdW mode representations as per fig. 8 and 9.

c) C_{3v} cluster 6_o^1 contributions tabulated relative to C_s cluster 6_o^1 vibronic origin as in fig. 13.

FIGURE CAPTIONS

Figure 1 — Mass selective $S_1 \leftarrow S_o$ spectrum and calculated ground state vdW modes of benzene$(Ar)_1$. Energy scale is relative to benzene$(Ar)_1$ 6_o^1 transition (38587.6 cm^{-1}). Nozzle backing conditions: P_o = 100 psig, T_o = 300 k. Peak positions and assignments as per Table I and fig. 2.

Figure 2 — Calculated ground state minimum energy configuration (a) and eigenvalue/eigenvector vdW modes (b)-(d) for benzene$(Ar)_1$. Cluster symmetry is C_{6v} with an equilibrium intermolecular distance of 3.45 Å. Eigenvectors are normalized and displayed at 2x magnification (2 Å total displacement).

Figure 3 — z-direction (vdW stretch) potential energy mapping of benzene$(Ar)_1$. Coordinate system is as shown in fig. 2. Translation is along z axis with x and y coordinates at equilibrium intermolecular distance values. Translation is displayed relative to equilibrium intermolecular distance, 3.45 Å. (6-12) potential energy mapping is represented by o; Taylor series expansion and energy levels are represented by —; Morse fit potential energy curve is represented by ---. Vibrational mode constants as per Table II.

Figure 4 — x(y)-direction (2-fold degenerate vdW bend) potential energy mapping of benzene$(Ar)_1$. Coordinate system is as shown in fig. 2. Translation is along x(y) axis with z and y(x) coordinates at equilibrium intermolecular distance values.

Translation is displayed relative to equilibrium intermolecular distance 3.45 Å. 6-12 potential energy mapping is represented by o; Taylor series expansion and energy levels are represented by —; Morse fit potential energy curve is represented by ---. Vibrational mode constants as per Table II.

Figure 5 Calculated ground state minimum energy configuration (a) and eigenvalue/eigenvector vdW modes (b)-(d) for s-tetrazine$(Ar)_1$. Cluster symmetry is C_{2v} with an equilibrium intermolecular distance of 3.45 Å. Eigenvectors are normalized and displayed at 2x magnification (2 Å total displacement).

Figure 6 Calculated ground state minimum energy configuration (a) and eigenvalue/eigenvector vdW modes (b)-(g) for benzene$(CH_4)_1$. Cluster symmetry is C_{3v} with an equilibrium intermolecular distance of 3.47 Å. Eigenvectors are normalized and displayed at 2x magnification (2 Å total displacement).

Figure 7 Calculated ground state minimum energy configuration (a) and eigenvalue/eigenvector vdW modes (b)-(g) for benzene$(H_2O)_1$. Cluster symmetry is C_s with an equilibrium intermolecular distance of 3.15 Å. Eigenvectors are normalized and displayed at 2x magnification (2 Å total displacement).

Figure 8 Calculated ground state minimum energy configuration (a) and eigenvalue/eigenvector vdW modes (b)-(g) for benzene$(NH_3)_1$. Cluster symmetry is C_{3v} with an equilibrium intermolecular distance of 3.23 Å. Eigenvectors are normalized and displayed at 2x magnification (2 Å total displacement).

Figure 9 Calculated ground state minimum energy configuration (a) and eigenvalue/eigenvector vdW modes (b)-(g) for benzene$(NH_3)_1$. Cluster symmetry is C_s with an equilibrium intermolecular distance of 3.29 Å. Eigenvectors are normalized and displayed at 2x magnification (2 Å total displacement).

Figure 10 Schematic $^1B_{3u} \leftarrow {}^1A_g$ spectrum (from ref. 5) and calculated ground state vdW modes of s-tetrazine$(Ar)_1$. Energy scale is relative to s-tetrazine$(Ar)_1$ 0_o^o transition (18104.9 cm^{-1}). Relative feature intensities are not shown. Feature positions and assignments as per Table III and fig. 5. vdW bends are represented by b_i in schematic spectrum (see text for explanation).

Figure 11 Mass selective $S_1 \leftarrow S_o$ spectrum (from ref. 2) and calculated ground state vdW modes of benzene$(CH_4)_1$. Energy scale is relative to benzene$(CH_4)_1$ 6_o^1 transition (38567.6 cm^{-1}). Feature positions and assignments as per Table IV and fig. 6.

Figure 12 Mass selective $S_1 \leftarrow S_o$ spectra (from ref. 3) and calculated ground state vdW modes of benzene$(H_2O)_1$. Energy scale is relative to benzene$(H_2O)_1$ 0_o^o and 6_o^1 transitions (38168.6 cm^{-1} and 38655.4 cm^{-1}, respectively). Feature positions and assignments as per Table V and fig. 7. s_z and t_y vdW modes are not shown.

Figure 13 Mass selective $S_1 \leftarrow S_o$ spectrum (from ref. 3) and calculated ground state vdW modes of benzene$(NH_3)_1$. Energy scale is

relative to benzene$(NH_3)_1$ 0_0^0 and 6_0^1 transitions for C_s cluster (38021.1 cm^{-1} and 38514.7 cm^{-1}, respectively). Feature positions and assignments as per Table VI and fig. 8 and 9. C_{3v} cluster s_z and t_{xy} modes are not shown.

Figure 14 z-direction (vdW stretch) potential energy mapping of benzene$(Ar)_1$ and $\beta = \frac{6}{R_o}$ Morse fit. Translation is relative to equilibrium intermolecular distance, 3.45 Å. (6-12) potential energy mapping using data set from ref. 9 is represented by o; Taylor series expansion and energy levels are represented by —; $\beta = \frac{6}{R_o}$ Morse fit potential energy curve is represented by ---. Taylor series vibrational mode constants as per Table II. $\beta = \frac{6}{R_o}$ Morse fit vibrational constants are $\omega_e = 47.22$ cm^{-1} $\omega_e\chi_e = 1.94$ cm^{-1}.

Figure 15 z-direction (vdW stretch) potential energy mapping of benzene$(Ar)_1$ and $\beta = \frac{6}{R_o}$ Morse fit. Translation is relative to equilibrium intermolecular distance, 3.5 Å. (6-12) potential energy mapping using data set from ref. 1 is represented by o; Taylor series expansion and energy levels are represented by — with $\omega_e = 46.48$ cm^{-1} and $\omega_e\chi_e = 1.81$ cm^{-1}; $\beta = \frac{6}{R_o}$ Morse fit potential energy curve is represented by ---. $\beta = \frac{6}{R_o}$ Morse fit vibrational mode constants are $\omega_e = 54.84$ cm^{-1} $\omega_e\chi_e$ $= 1.90$ cm^{-1}.

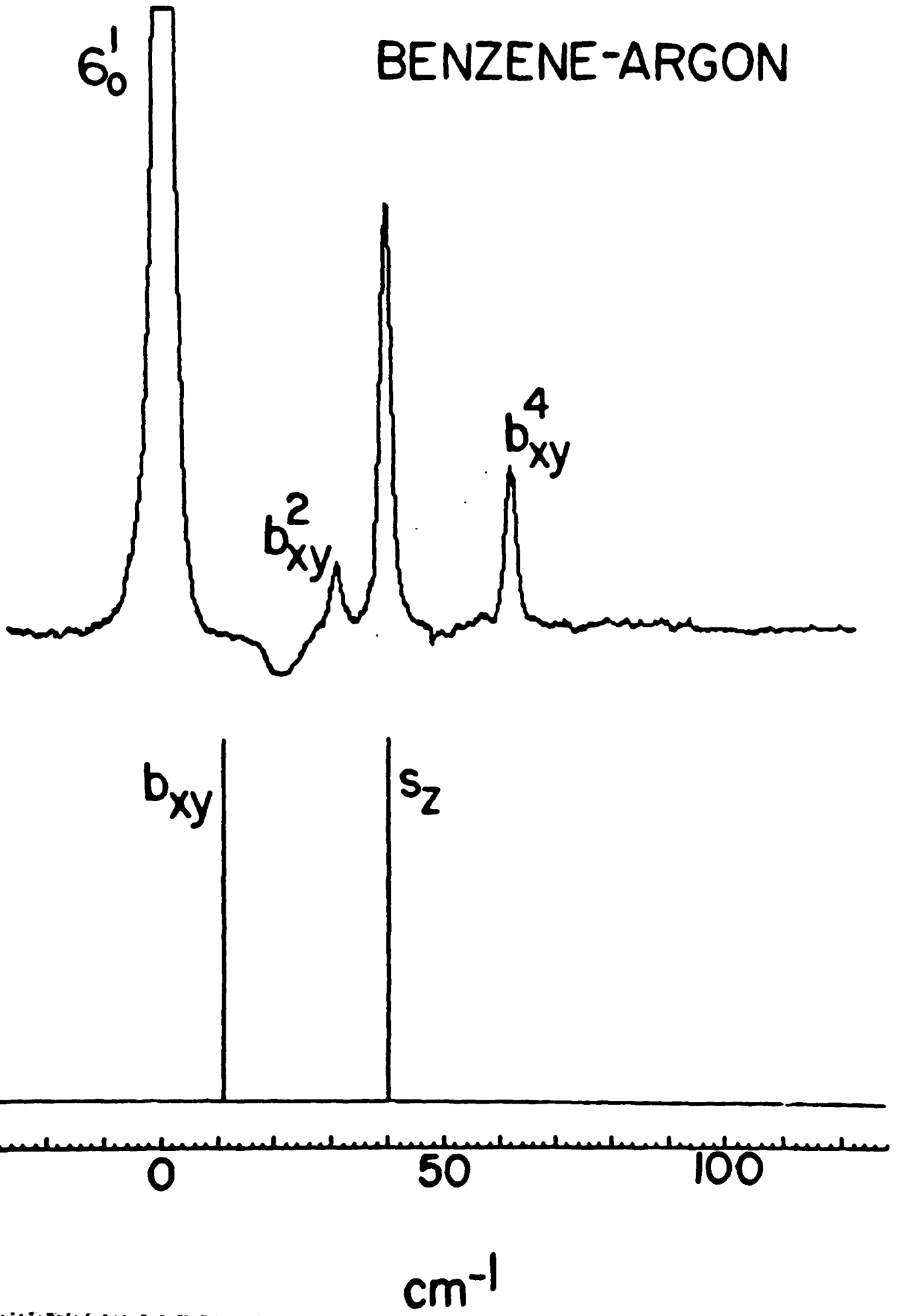
BENZENE-ARGON
6_0^1
b_{xy}^2
b_{xy}^4
b_{xy}
s_z
0
50
100
cm^{-1}

BENZENE-ARGON

C_{6v}

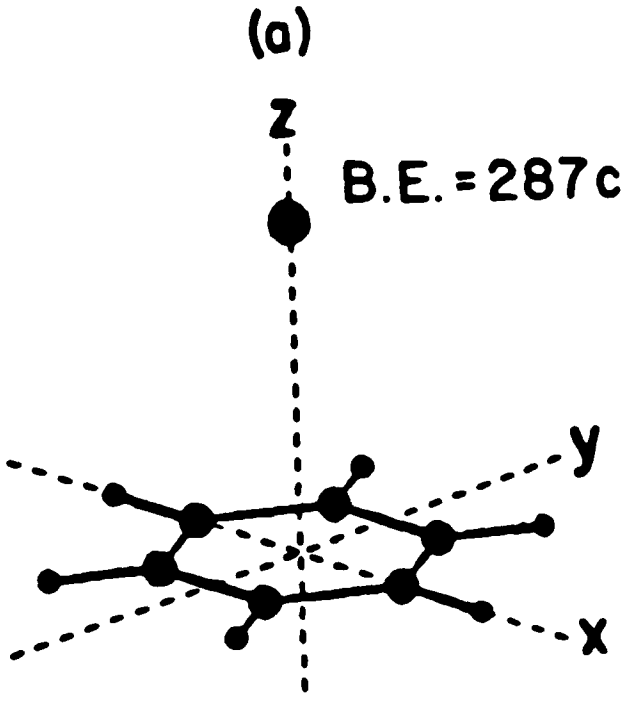

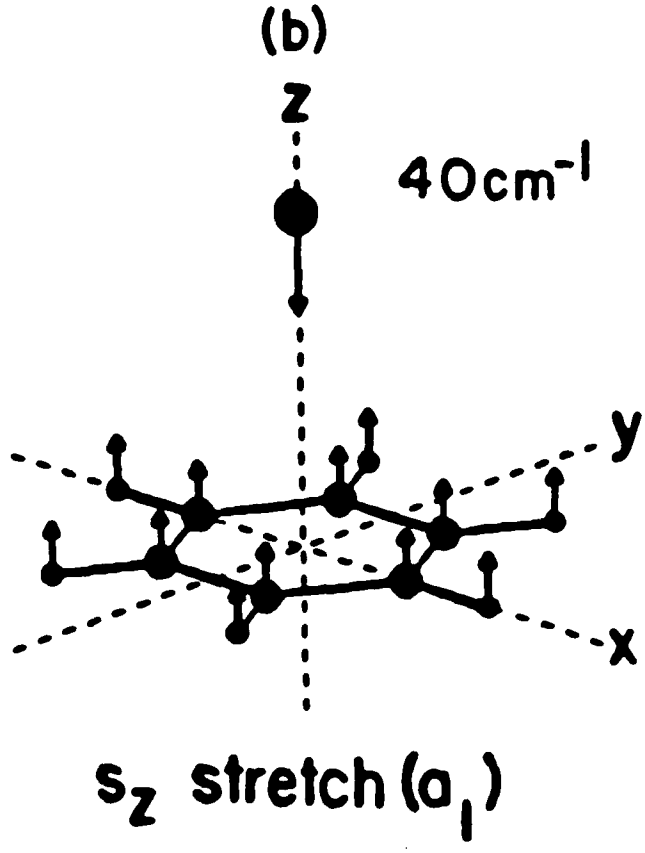

s_z stretch (a_1)

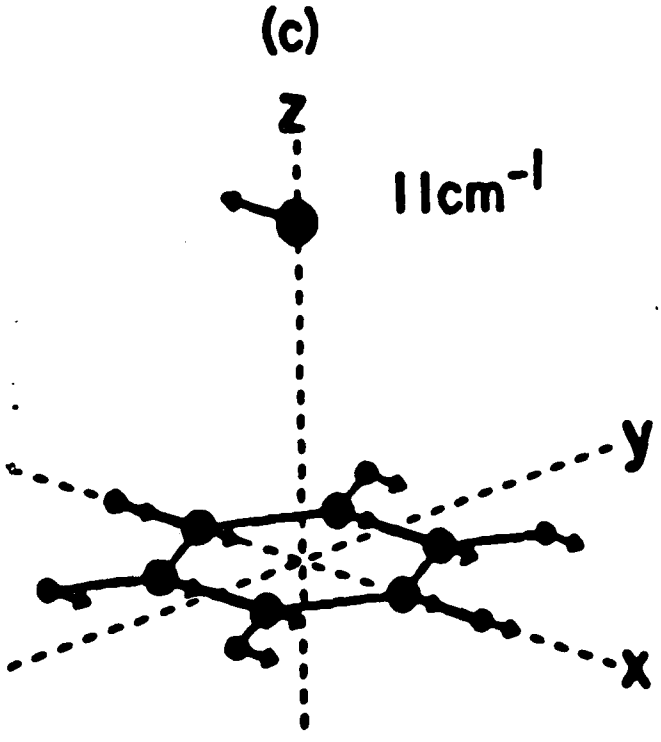

b_x bend (e_1)

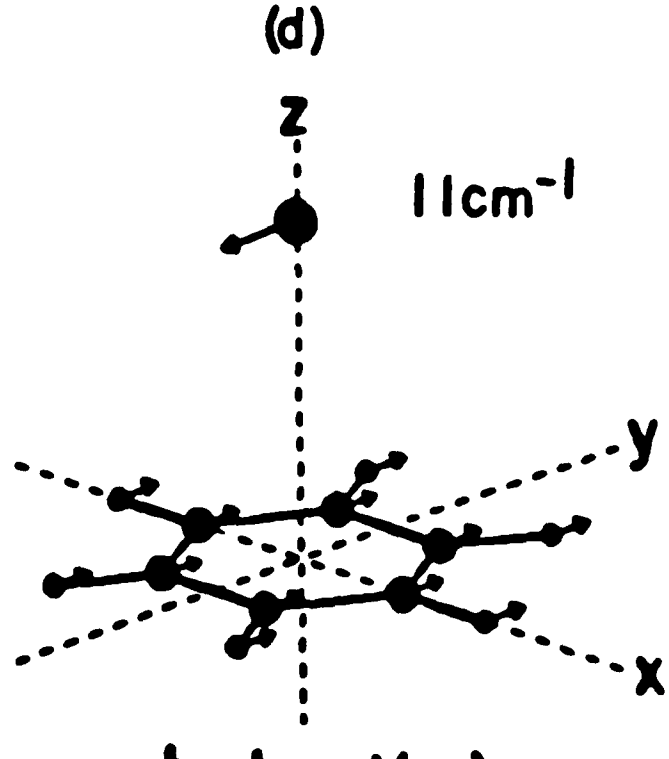

b_y bend (e_1)

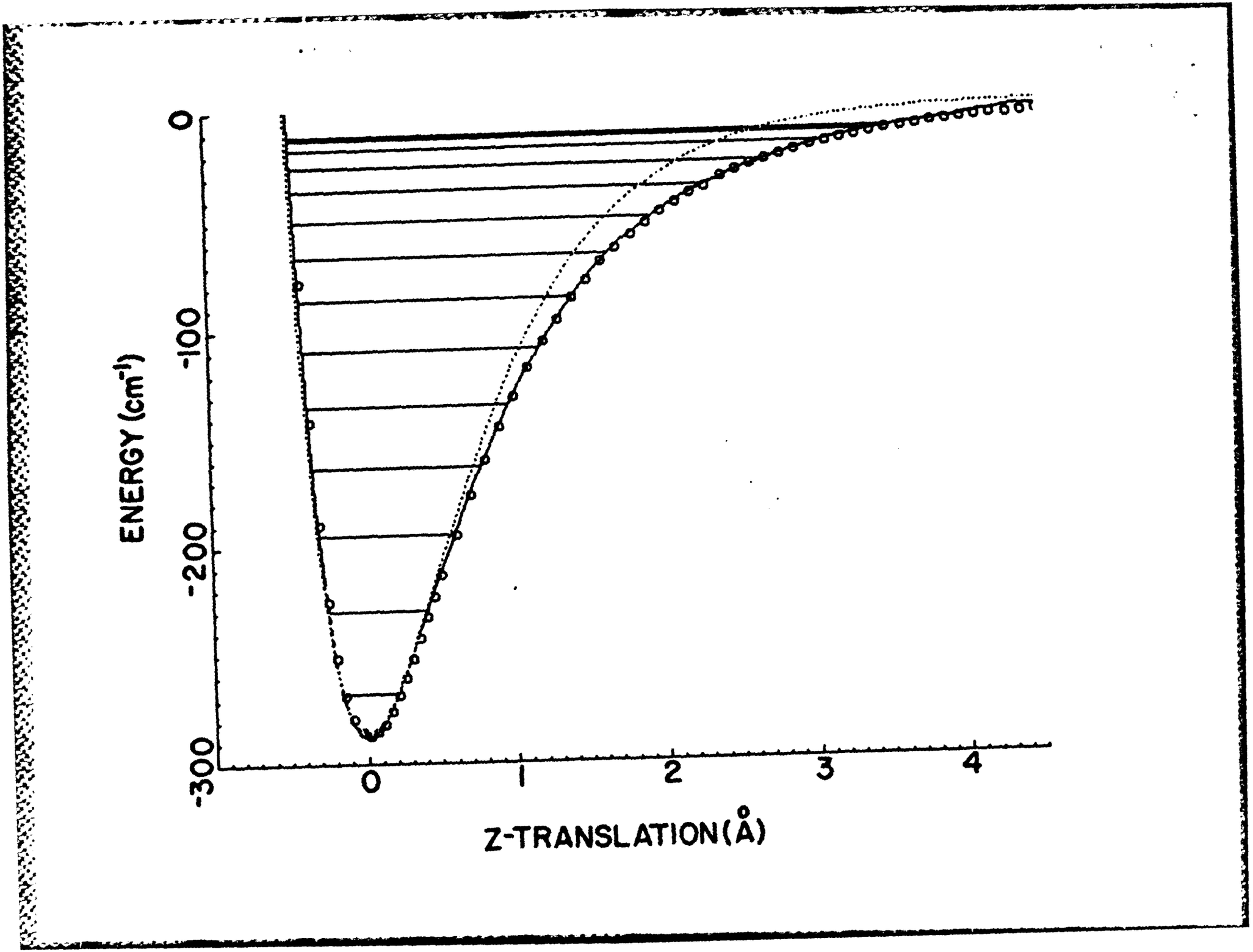
0
-100
-200
-300
ENERGY (cm⁻¹)
0
1
2
3
4
Z-TRANSLATION (Å)

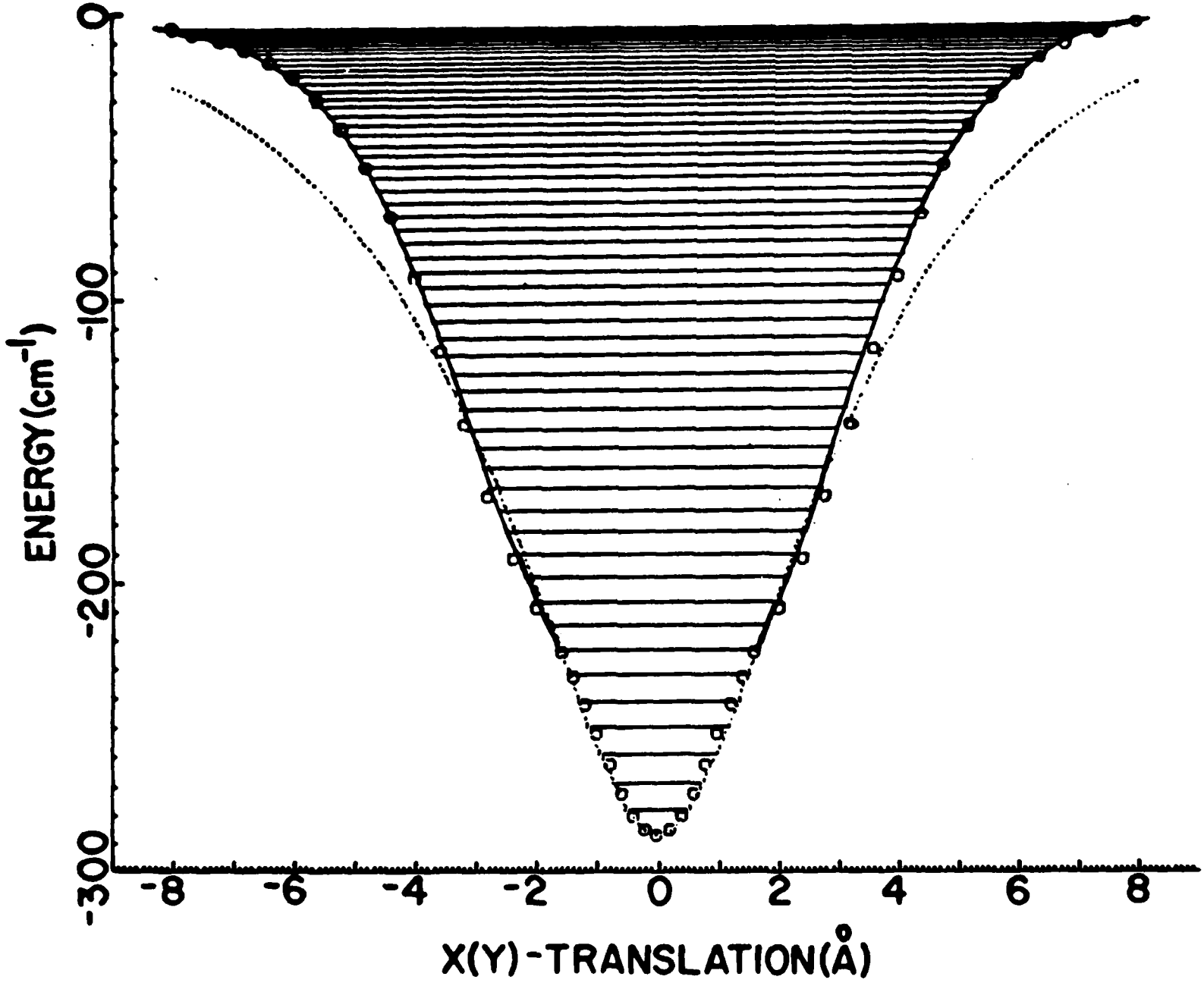
0
-100
-200
-300
ENERGY(cm⁻¹)
-8
-6
-4
-2
0
2
4
6
8
X(Y)-TRANSLATION(Å)

s-TETRAZINE-ARGON

C_{2v}

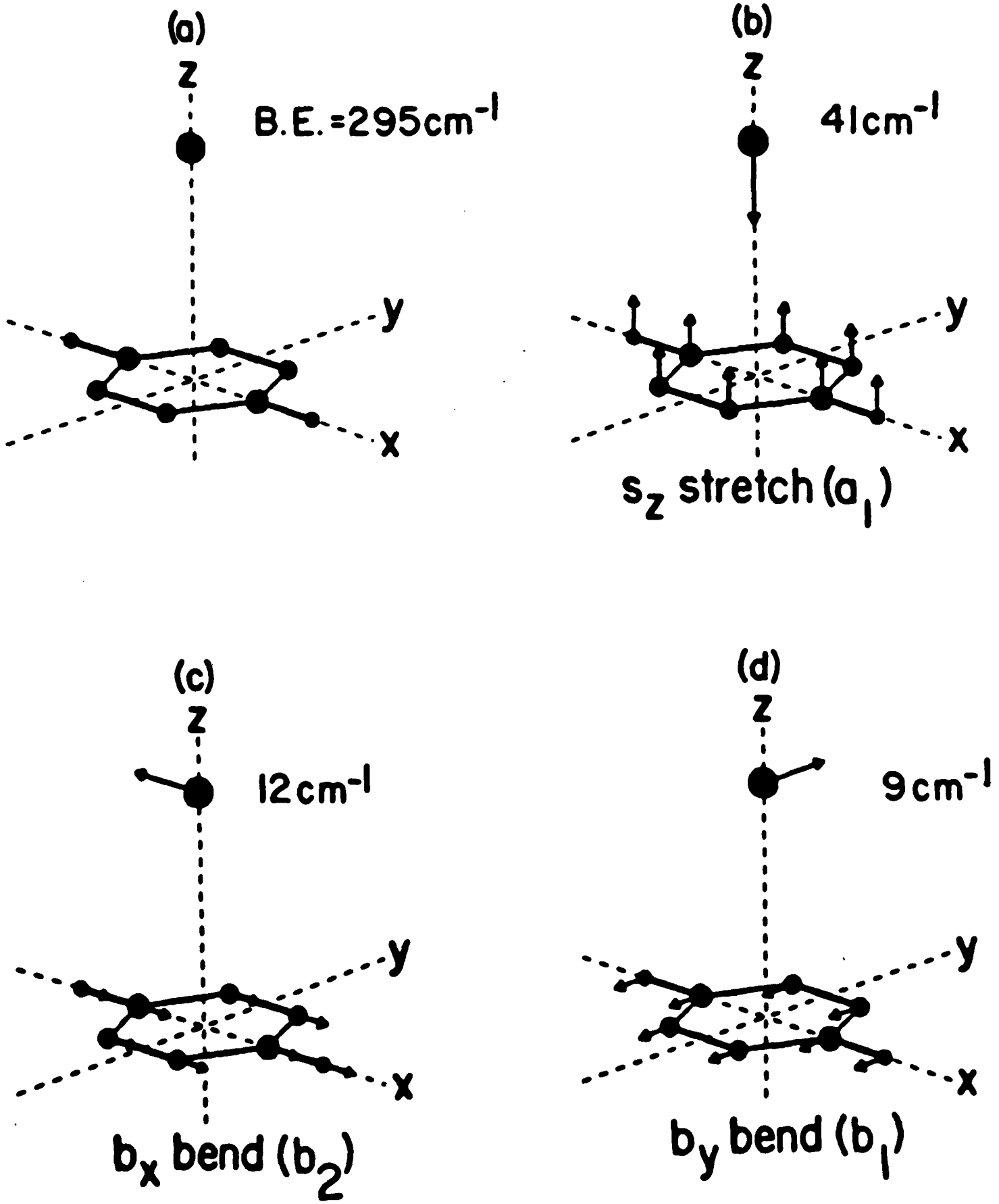

BENZENE-METHANE

C_{3v}

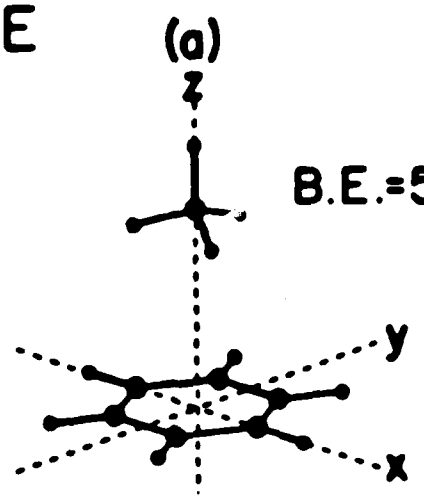

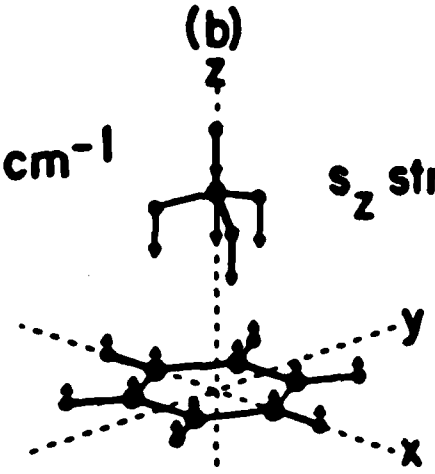

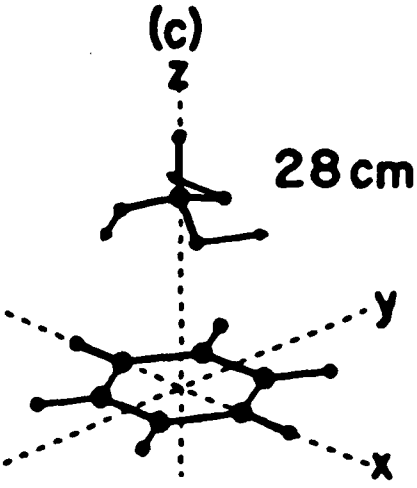

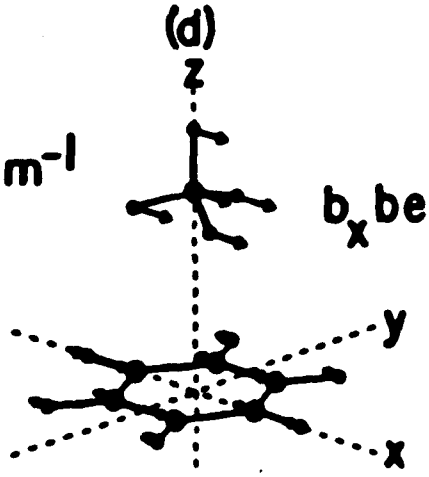

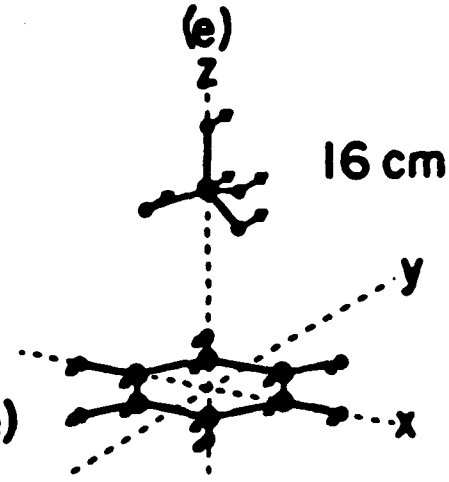

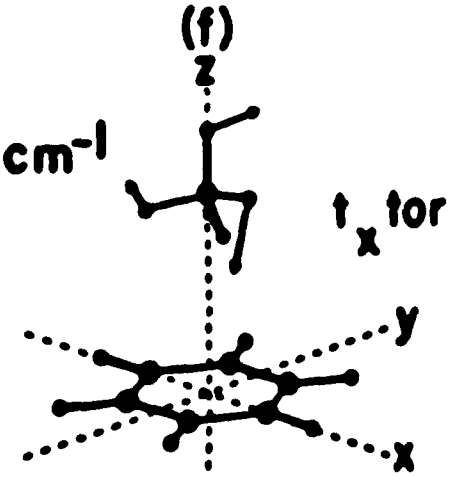

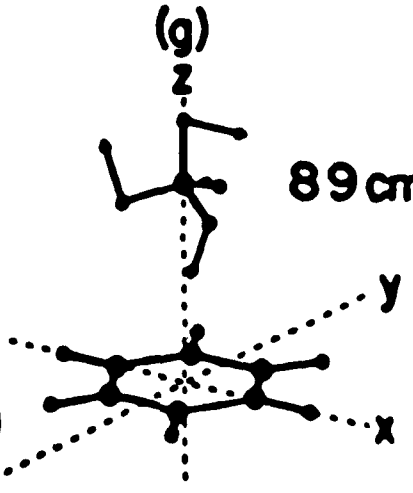

BENZENE-WATER

C_s

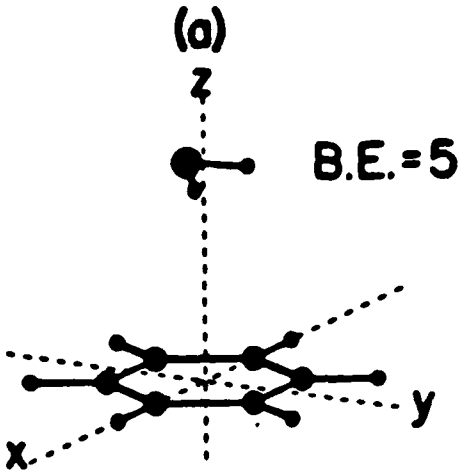

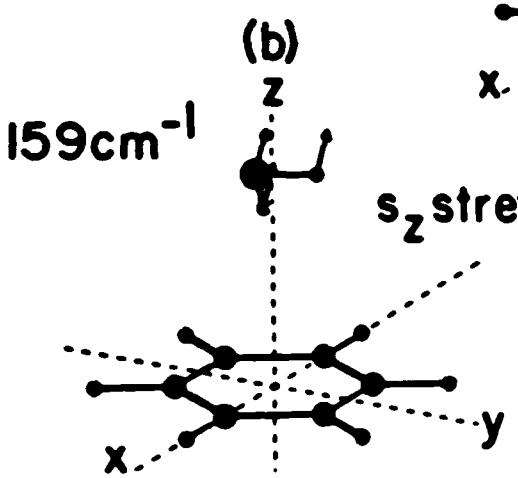

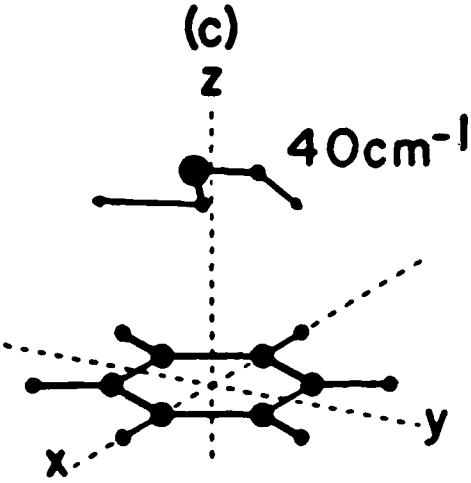

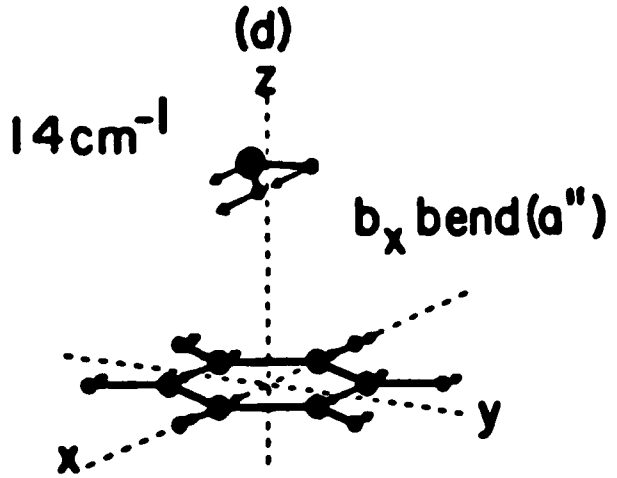

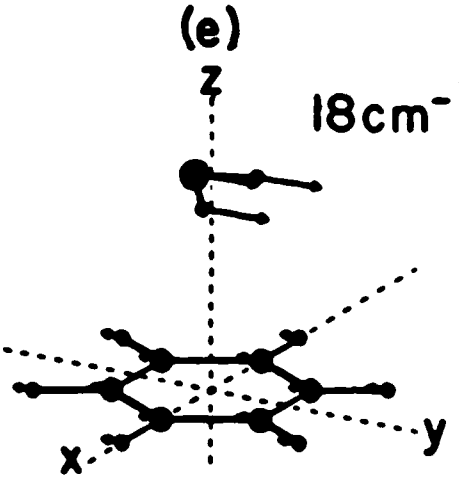

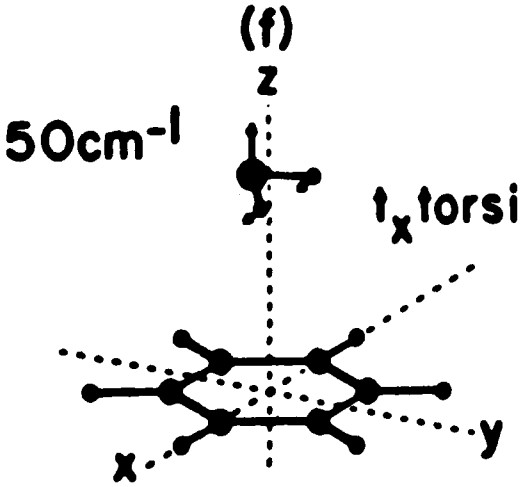

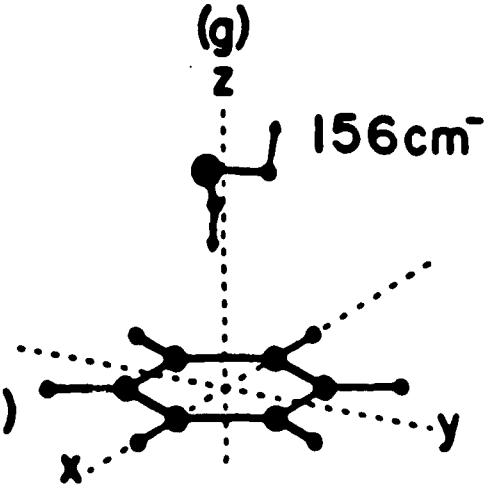

BENZENE-AMMONIA

C_{3v}

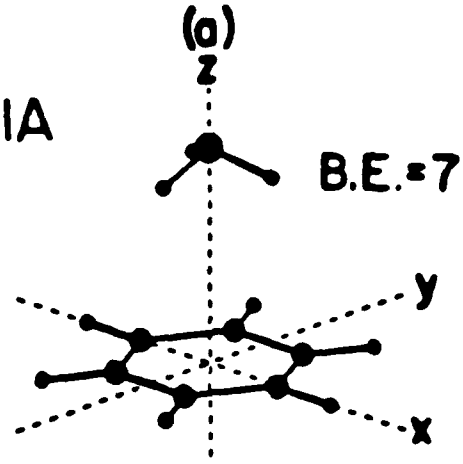

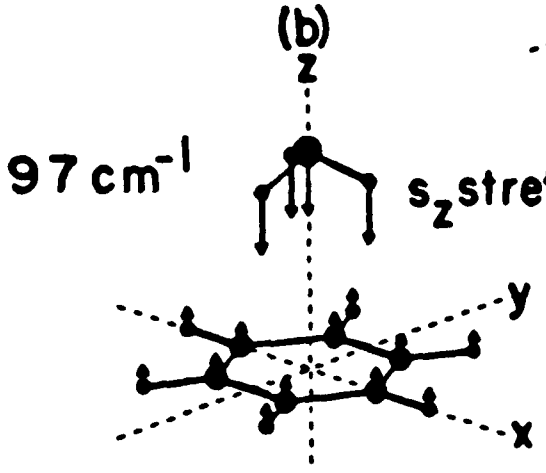

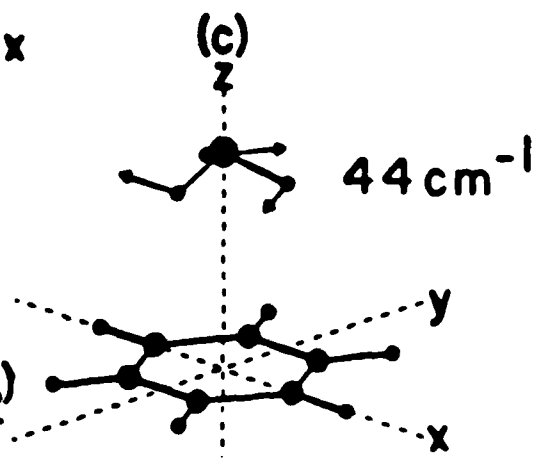

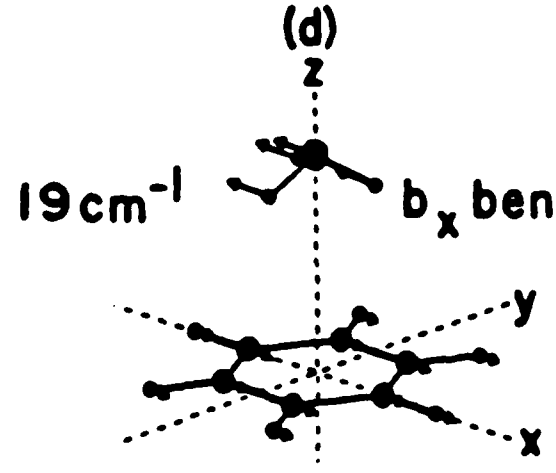

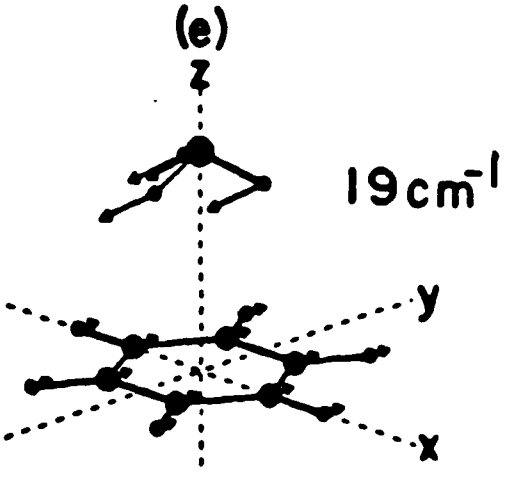

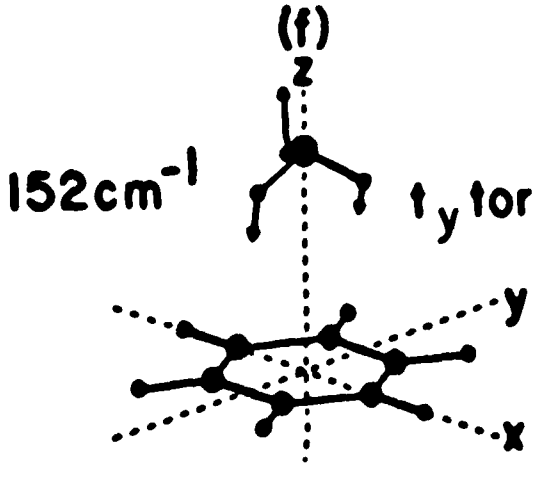

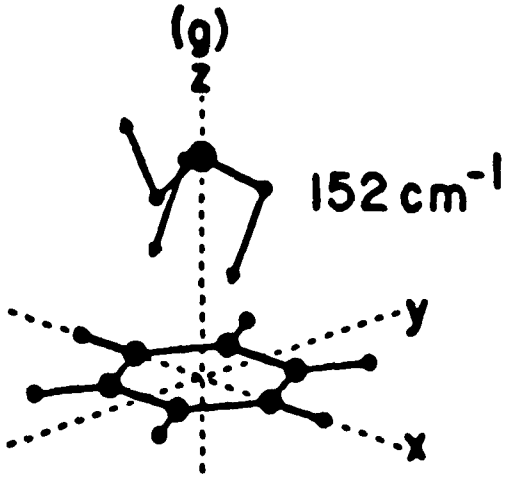

BENZENE-AMMONIA

C_s

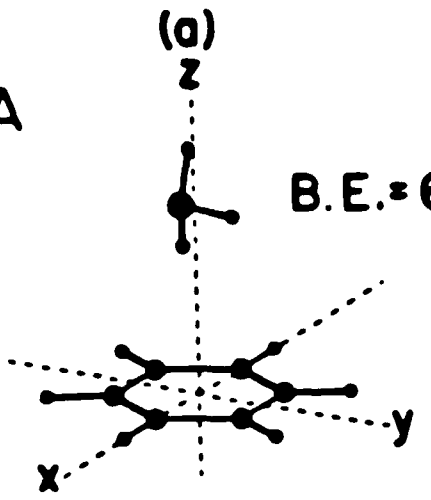

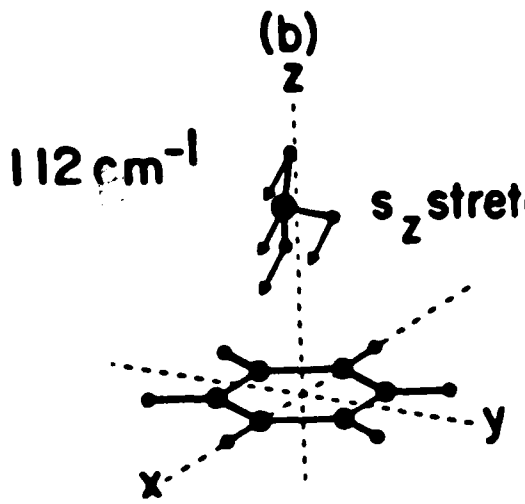

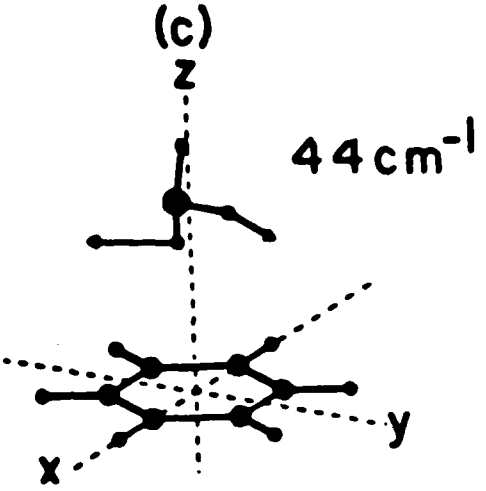

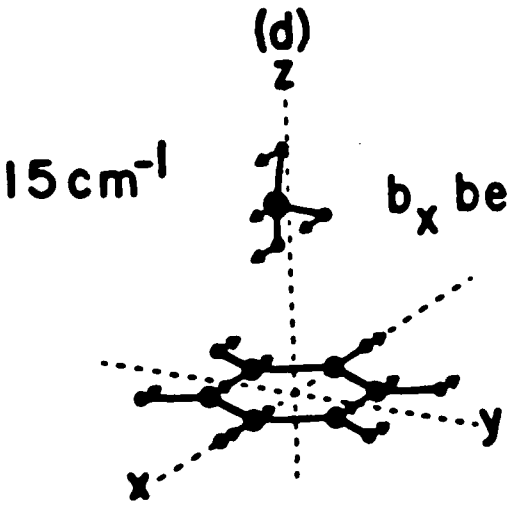

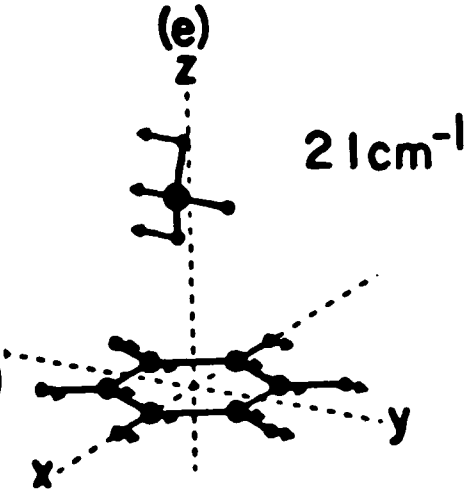

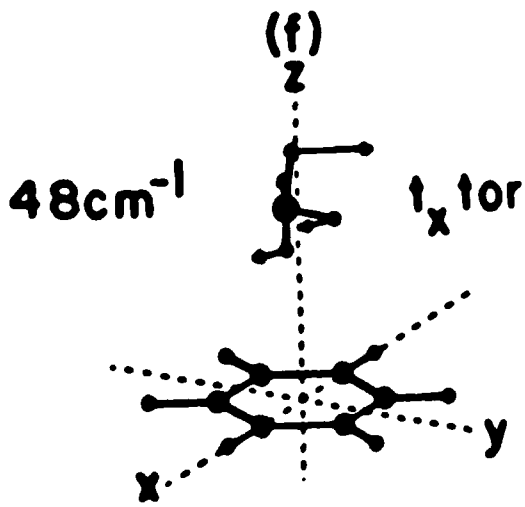

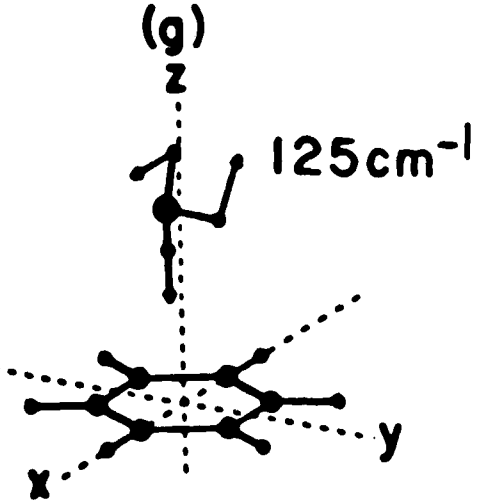

s-TETRAZINE-ARGON

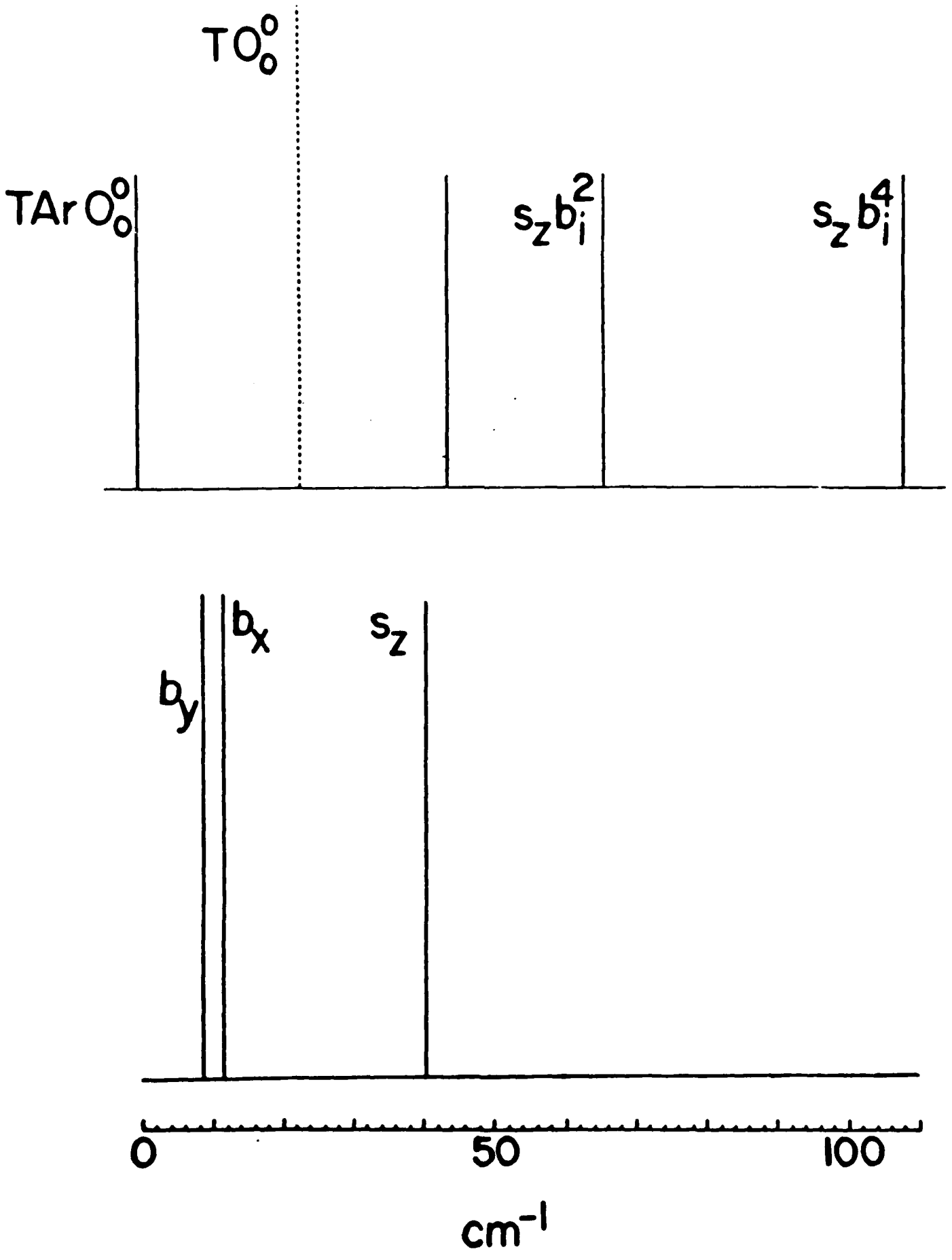

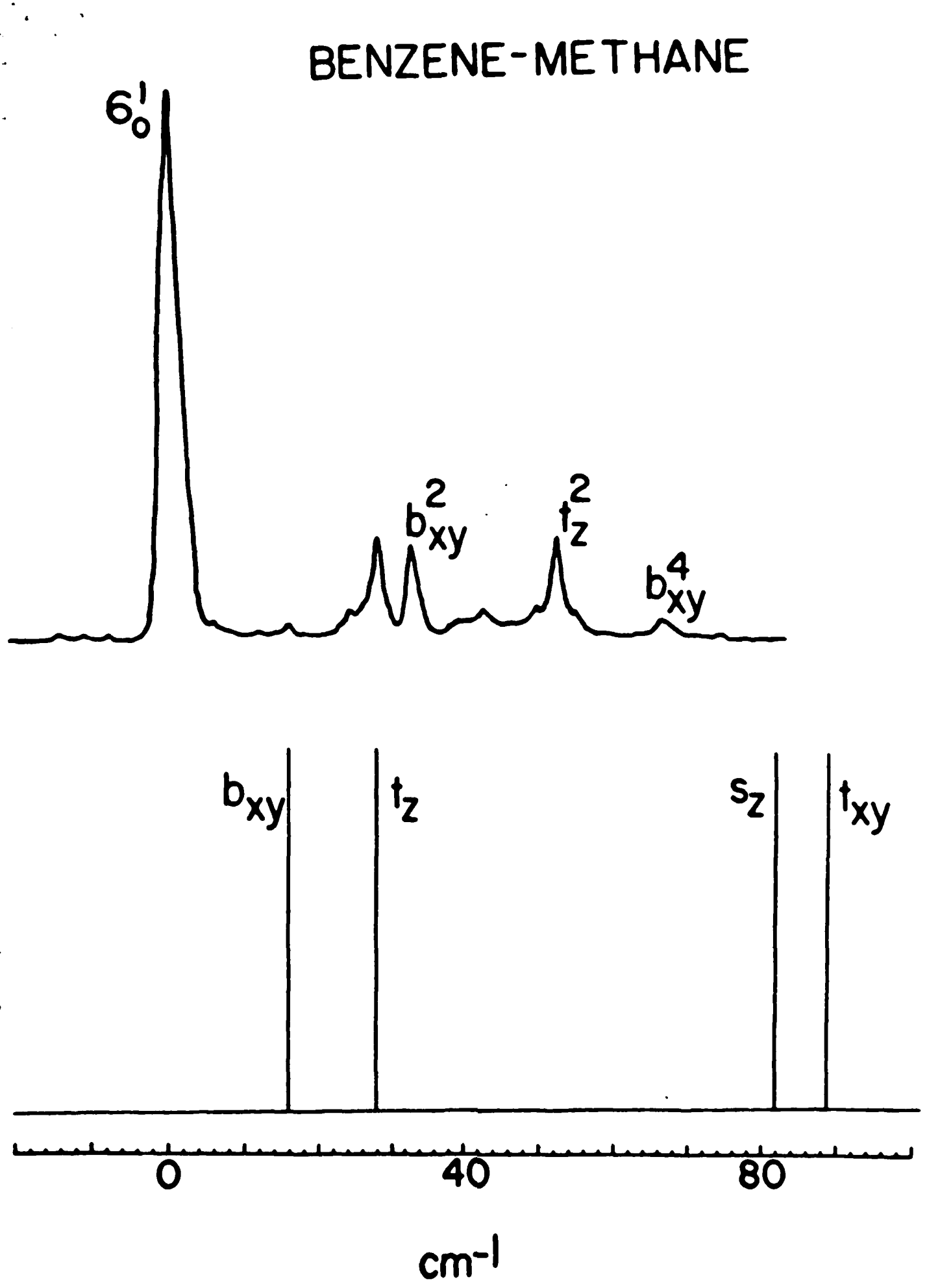
BENZENE-METHANE
6_0^1
b_{xy}^2
t_z^2
b_{xy}^4
b_{xy}
t_z
s_z
t_{xy}
0
40
80
cm⁻¹

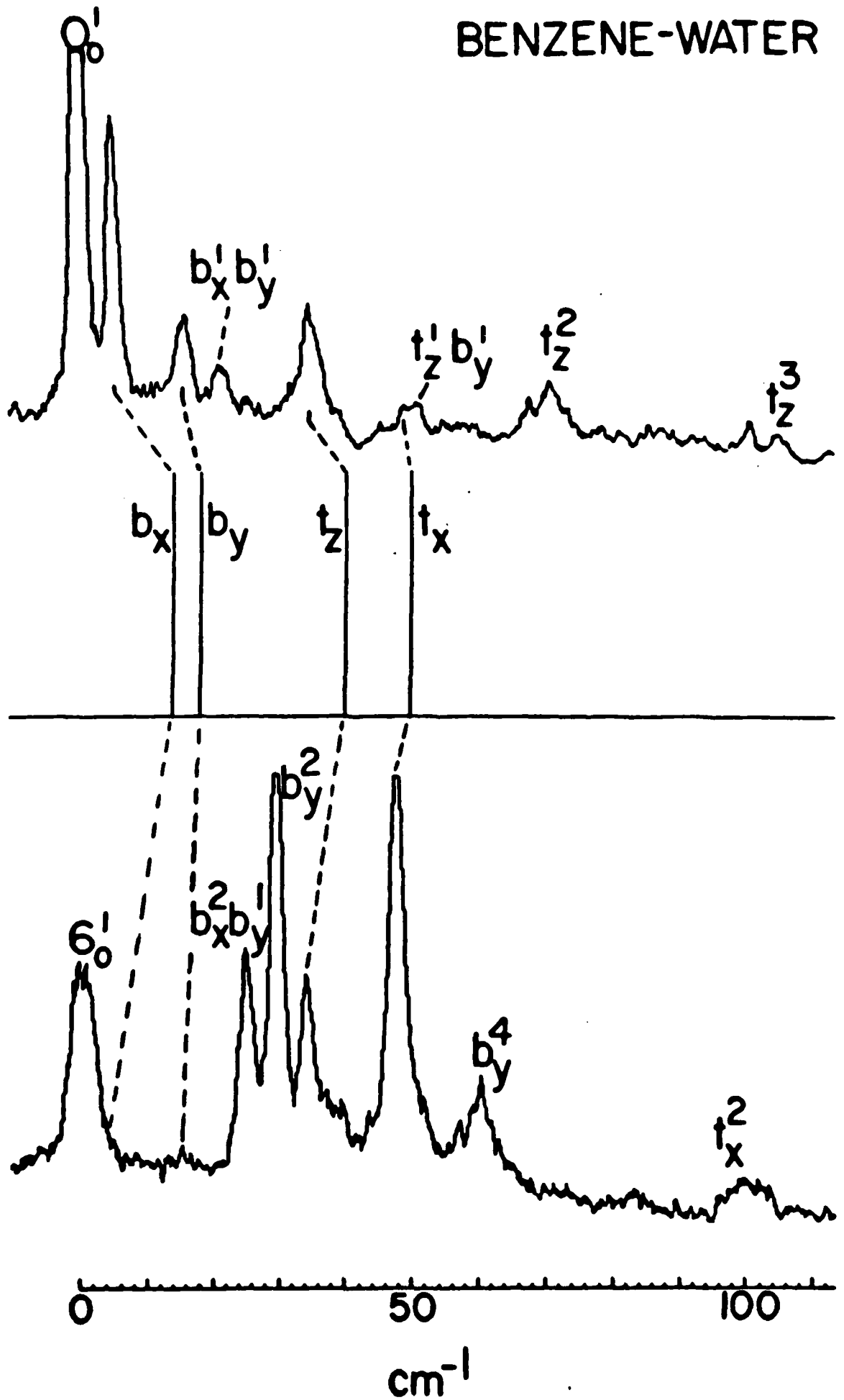
BENZENE-WATER
0_0^1
b_x^1 b_y^1
t_z^1 b_y^1
t_z^2
t_z^3
b_x
b_y
t_z
t_x
b_y^2
6_0^1
$b_x^2 b_y^1$
b_y^4
t_x^2
0
50
100
cm^{-1}

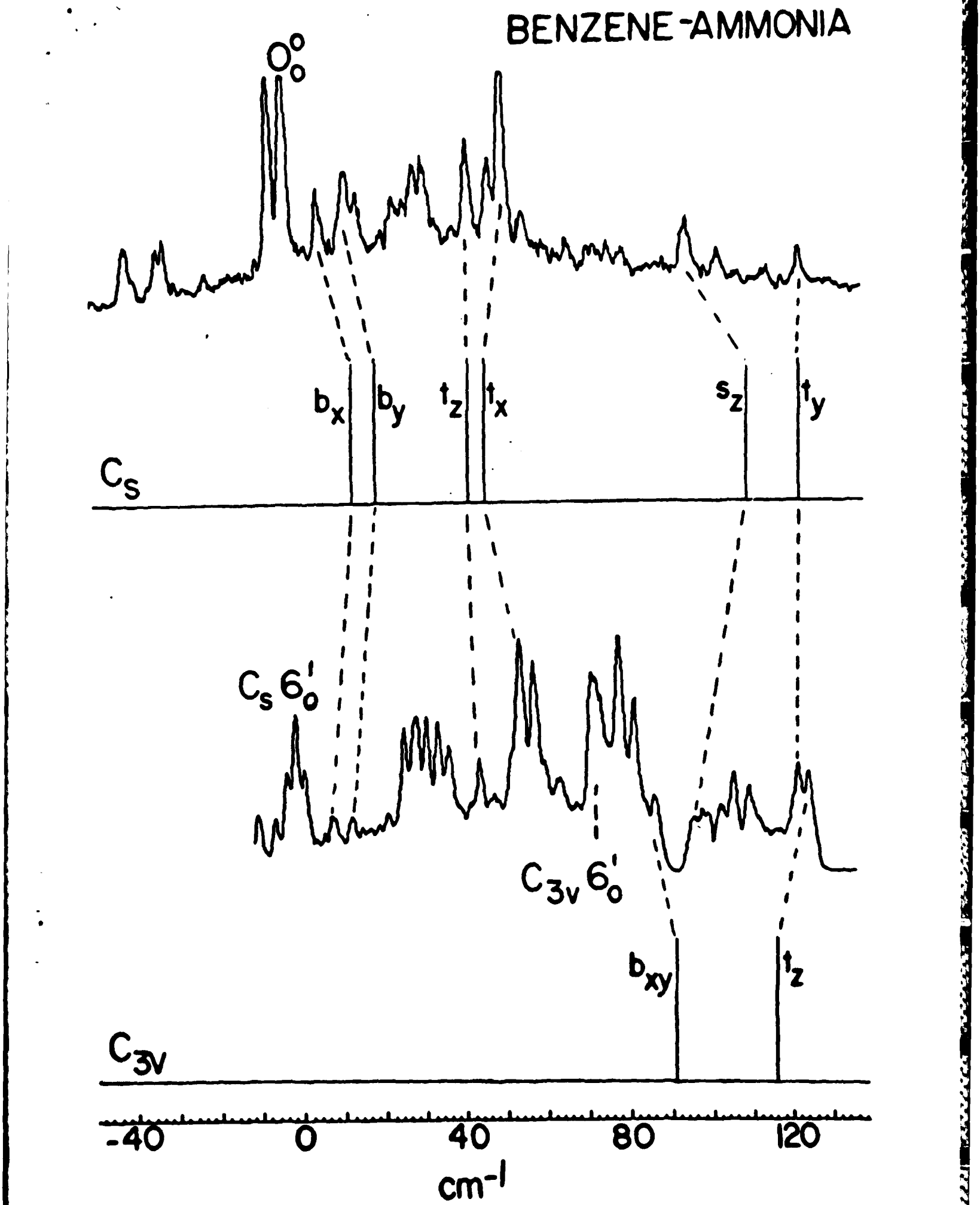
BENZENE-AMMONIA
0_0^0
b_x
b_y
t_z
t_x
s_z
t_y
C_s
$C_s\,6_0'$
$C_{3v}\,6_0'$
b_{xy}
t_z
C_{3v}
-40
0
40
80
120
cm^{-1}

ENERGY (cm⁻¹)
0
-100
-200
-300
Z-TRANSLATION(Å)
0
1
2
3
4

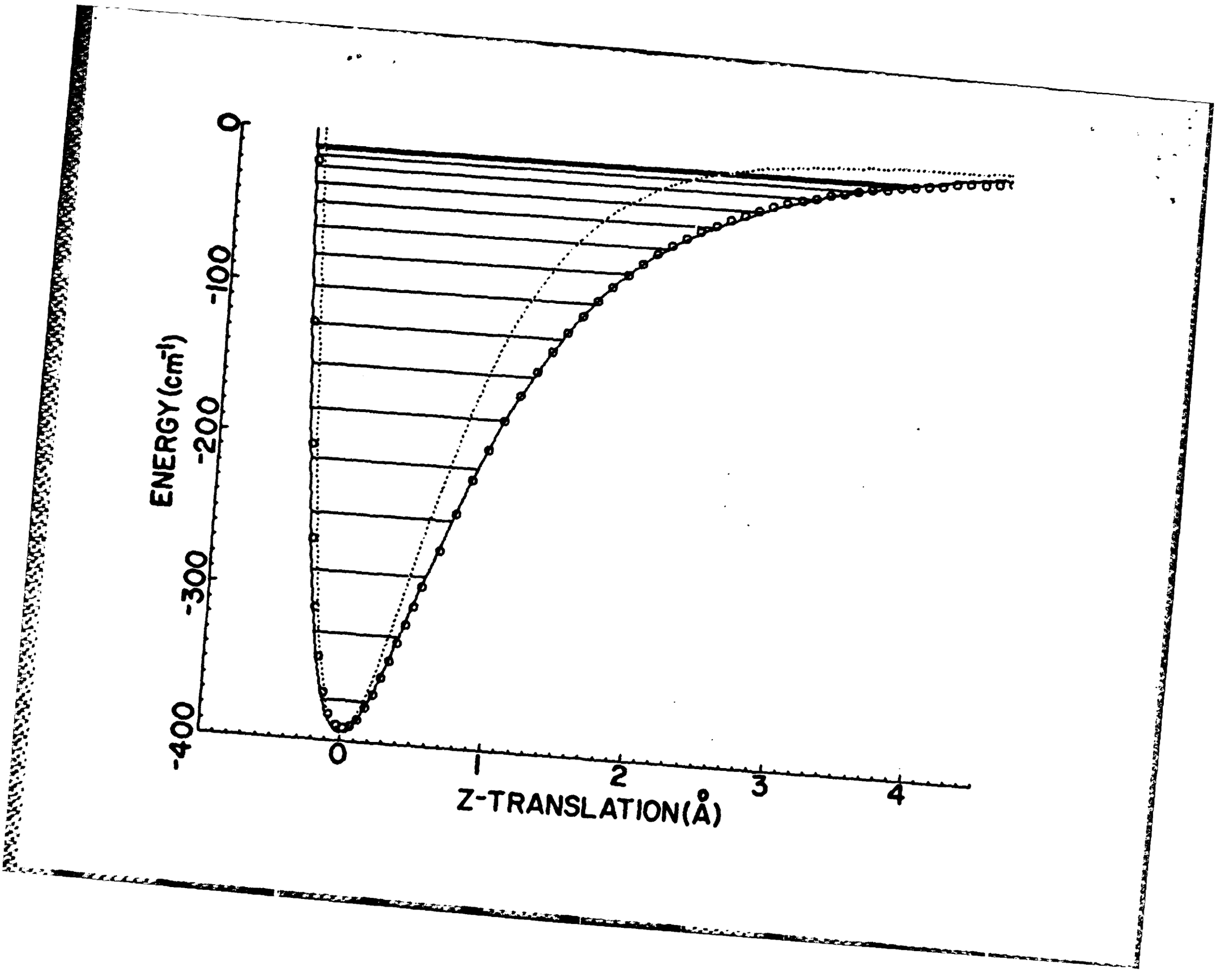
ENERGY (cm⁻¹)
0
-100
-200
-300
-400
0
1
2
3
4
Z-TRANSLATION (Å)

DL/413/83/01
GEN/413-2

TECHNICAL REPORT DISTRIBUTION LIST, GEN

	No. Copies
Office of Naval Research Attn: Code 413 800 N. Quincy Street Arlington, Virginia 22217	2
Dr. Bernard Douda Naval Weapons Support Center Code 5042 Crane, Indiana 47522	1
Commander, Naval Air Systems Command Attn: Code 310C (H. Rosenwasser) Washington, D.C. 20360	1
Naval Civil Engineering Laboratory Attn: Dr. R. W. Drisko Port Hueneme, California 93401	1
Defense Technical Information Center Building 5, Cameron Station Alexandria, Virginia 22314	12
DTNSRDC Attn: Dr. G. Bosmajian Applied Chemistry Division Annapolis, Maryland 21401	1
Dr. William Tolles Superintendent Chemistry Division, Code 6100 Naval Research Laboratory Washington, D.C. 20375	1
Dr. David Young Code 334 NORDA NSTL, Mississippi 39529	1
Naval Weapons Center Attn: Dr. A. B. Amster Chemistry Division China Lake, California 93555	1
Scientific Advisor Commandant of the Marine Corps Code RD-1 Washington, D.C. 20380	1
U.S. Army Research Office Attn: CRD-AA-IP P.O. Box 12211 Research Triangle Park, NC 27709	1
Mr. John Boyle Materials Branch Naval Ship Engineering Center Philadelphia, Pennsylvania 19112	1
Naval Ocean Systems Center Attn: Dr. S. Yamamoto Marine Sciences Division San Diego, California 91232	1

DL/413/83/01
051A/413-2

ABSTRACTS DISTRIBUTION LIST, 051A

Dr. M. A. El-Sayed
Department of Chemistry
University of California
Los Angeles, California 90024

Dr. E. R. Bernstein
Department of Chemistry
Colorado State University
Fort Collins, Colorado 80521

Dr. J. R. MacDonald
Chemistry Division
Naval Research Laboratory
Code 6110
Washington, D.C. 20375

Dr. G. B. Schuster
Chemistry Department
University of Illinois
Urbana, Illinois 61801

Dr. W. M. Jackson
Department of Chemistry
Howard University
Washington, D.C. 20059

Dr. M. S. Wrighton
Department of Chemistry
Massachusetts Institute of Technology
Cambridge, Massachusetts 02139

Dr. A. Paul Schaap
Department of Chemistry
Wayne State University
Detroit, Michigan 49207

Dr. Gary Bjorklund
IBM
5600 Cottle Road
San Jose, California 95143

Dr. G. A. Crosby
Chemistry Department
Washington State University
Pullman, Washington 99164

Dr. W. E. Moerner
I.B.M. Corporation
5600 Cottle Road
San Jose, California 95193

Dr. Theodore Pavlopoulos
NOSC
Code 5132
San Diego, California 91232

Dr. D. M. Burland
IBM
San Jose Research Center
5600 Cottle Road
San Jose, California 95143

Dr. John Cooper
Code 6170
Naval Research Laboratory
Washington, D.C. 20375

Dr. George E. Walrafen
Department of Chemistry
Howard University
Washington, D.C. 20059

Dr. Joe Brandelik
AFWAL/AADO-1
Wright Patterson AFB
Fairborn, Ohio 45433

Dr. Carmen Ortiz
Consejo Superior de
Investigaciones Cientificas
Serrano 117
Madrid 6, SPAIN

Dr. John J. Wright
Physics Department
University of New Hampshire
Durham, New Hampshire 03824

Dr. Kent R. Wilson
Chemistry Department
University of California
La Jolla, California 92093

END

10-86

DTIC